# *CALORIMETRY*

*Things every experimental particle physicist ought to know*
*(but unfortunately, few do)*

*Richard Wigmans*
*Texas Tech University*

*EDIT 2011*
*CERN, Feb. 2011*

# Calorimeters

- In particle physics, a calorimeter is a (massive) detector in which the particles to be detected are completely STOPPED

  The absorption process is usually referred to as "shower development"

- The detector is instrumented such as to provide signals that make it possible to determine the particle's 4-vector

- The signals may be provided by:

  - Scintillator: The total amount of light produced in the absorption process is a measure for the energy of the incoming particle
  - Liquid argon: The charge liberated in the stopping process provides the signals
  - Water: The Čerenkov light serves as the source of information

- The segmentation of the instrumented volume makes it possible to determine the momentum vector of the particles.
  The signals in the different calorimeter "towers" indicate the shower axis, and thus the direction of the incoming particle.

- The particle type may be derived from the shower profile, the time structure of the signals, ....

# *Why calorimetry?*

- Measure *charged + neutral* particles

- Obtain information on *energy flow*:
  Total (missing) transverse energy, jets, *etc.*

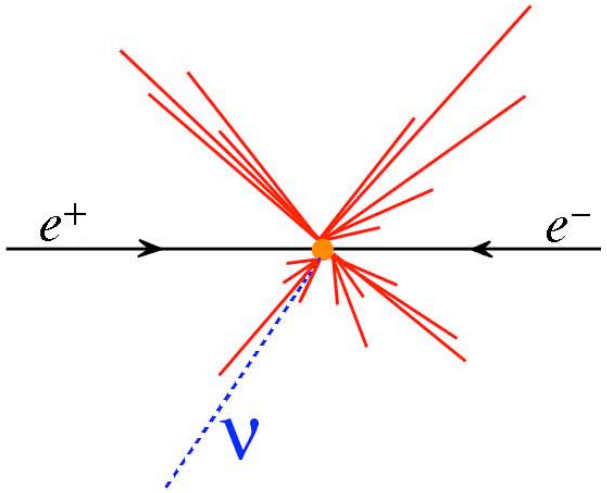


- Obtain information *fast*
  → recognize and select interesting events in real time *(trigger)*

- Performance of calorimeters *improves with energy*
  (~ $E^{-1/2}$ if statistical processes are the limiting factor)

*If* $E \propto$ *signal, i.e.* $E \propto$ *# signal quanta* $n \longrightarrow \sigma(E) \propto \sqrt{n}$

$\longrightarrow$ *energy resolution* $\dfrac{\sigma(E)}{E} \propto 1/\sqrt{n} \propto 1/\sqrt{E}$

# *In an ideal calorimeter, resolution scales as $E^{-1/2}$*

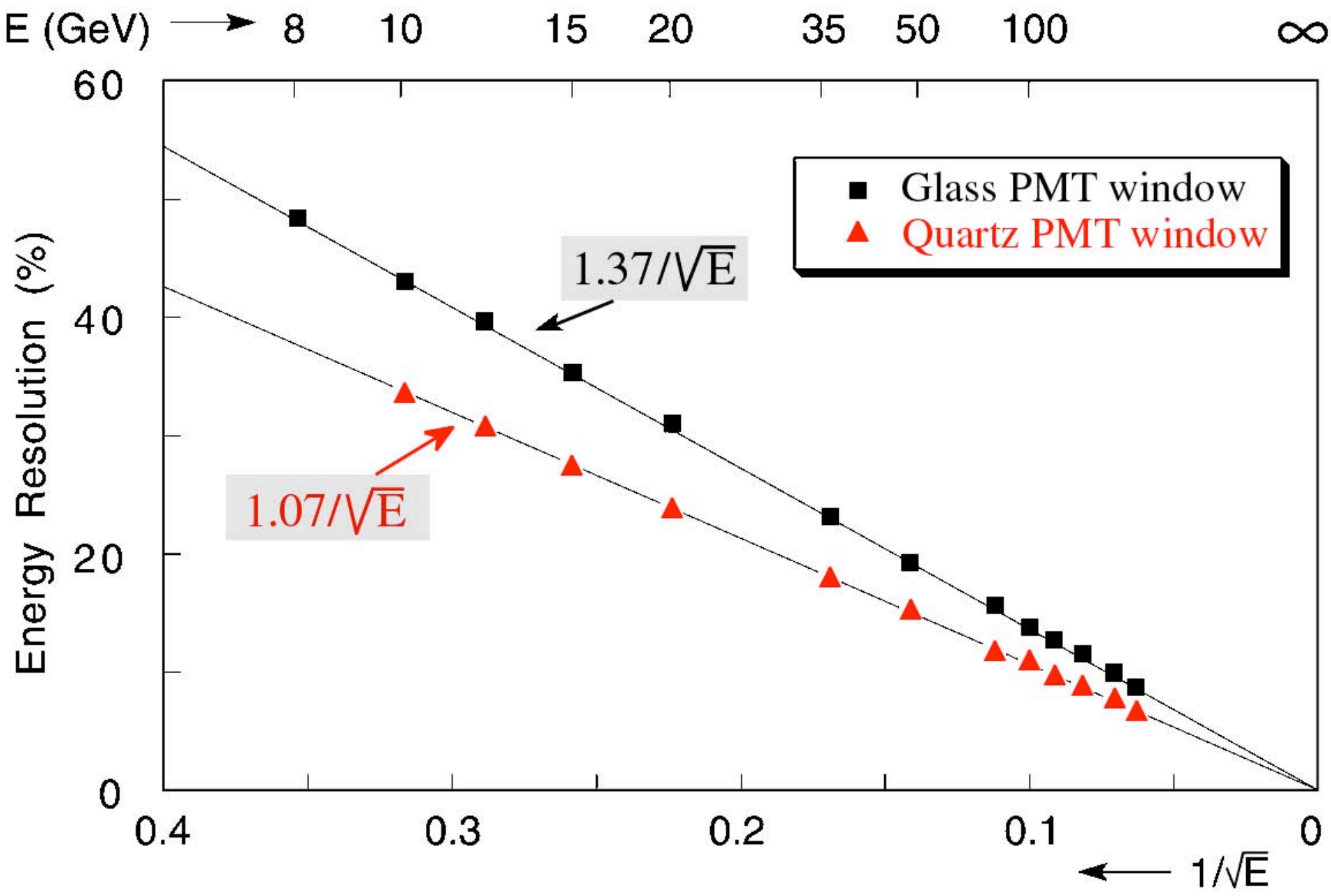

# *Energy resolution of a homogeneous hadron calorimeter*

*(60 tonnes of liquid scintillator)*

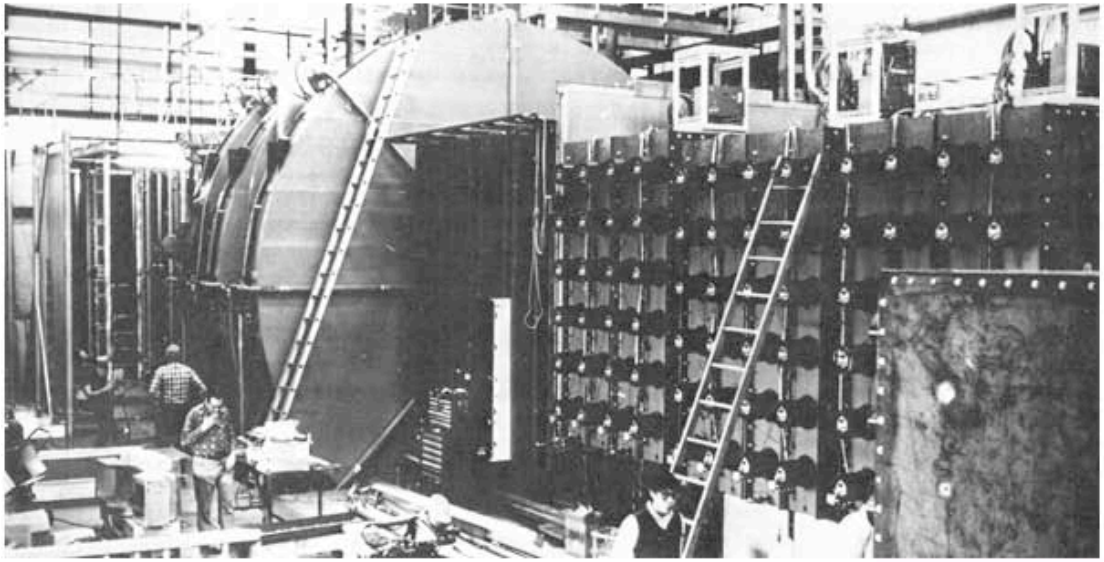

*Statistical processes are NOT the limiting factor here. Resolution is limited by fluctuations in invisible energy losses, related to e/h ~1.7*

*From:* NIM 125 (1975) 447

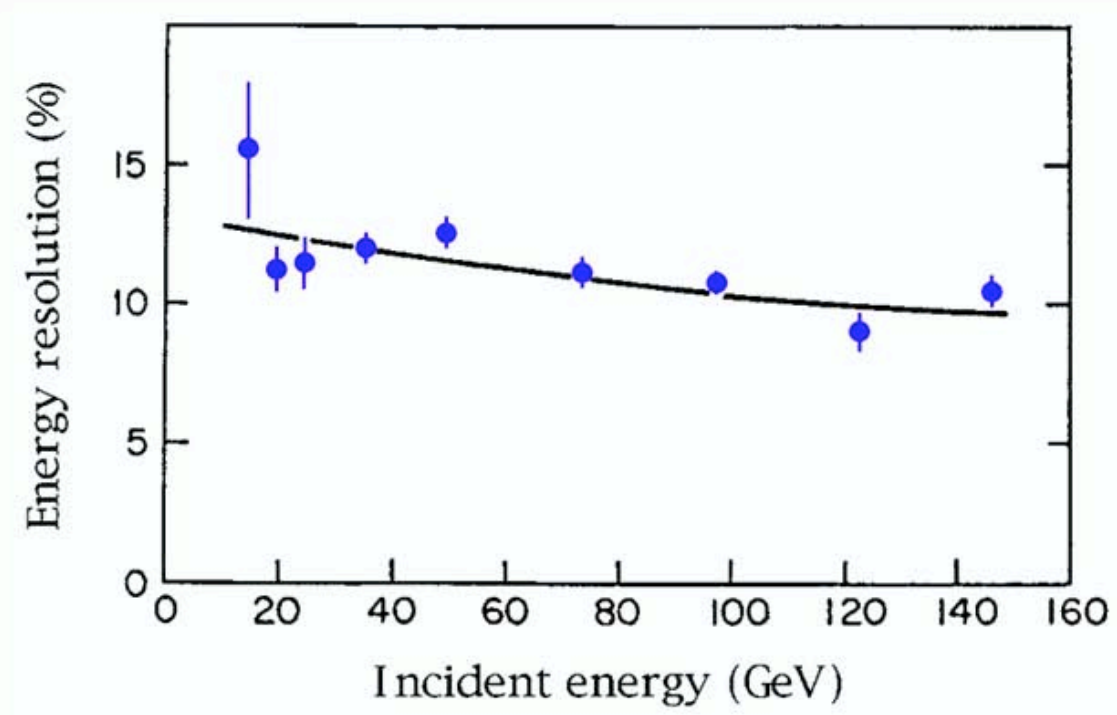

# *Important calorimeter features*

- Energy resolution
- Position resolution (need 4-vectors for physics)
- Signal speed
- Particle ID capability

*but also*

- *Gaussian response function* (avoid bias for steeply falling distributions)
- *Signal linearity*, or at least
- Well known relationship between signal & energy *(reliable calibration)*

*Most hadron calorimeters fall short in this respect*

*Signal generating mechanisms*

*Types of calorimeters*

# *Interactions of Particles and Matter*

## *Photoemission*

- Atomic excitation (followed by de-excitation)

*Particle loses energy by promoting an atomic electron to a higher energy state. When the electron falls back to the ground state, the energy may be released in the form of a photon.*

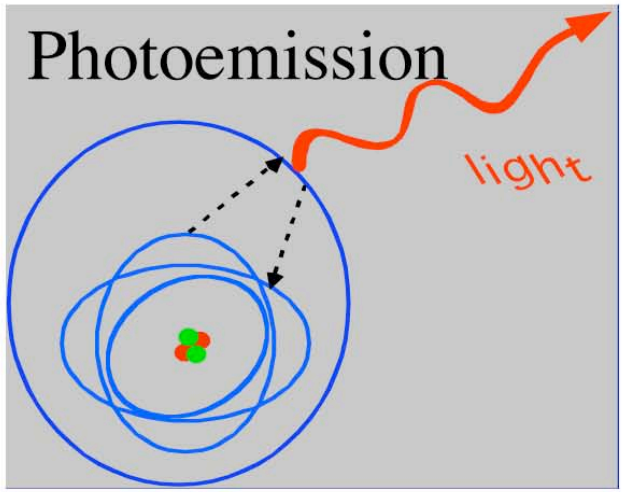

# *Interactions of Particles and Matter*

## *Ionization*

- *An atomic electron is knocked free from the atom as a result of the interaction with the charged particle's E field*
- *The remaining atom is now charged It is an ion*
- *The atom may be left in an excited state and emit a photon*

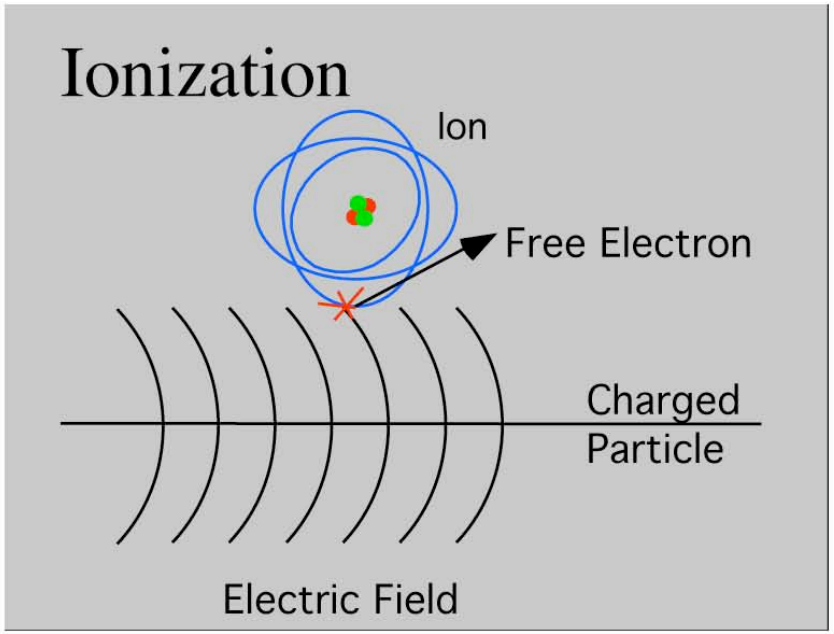

# *Interactions of Particles with Matter*

## *Collective effects*

- *The electric field of a particle may have a long-range interaction with material it traverses*

- *Čerenkov effect*

  *Turns on when the particle speed exceeds the medium's light speed:*

  $$v = \beta c > c/n$$

- *Light is emitted at the angle*

  $$\theta = \arccos(1/\beta n)$$

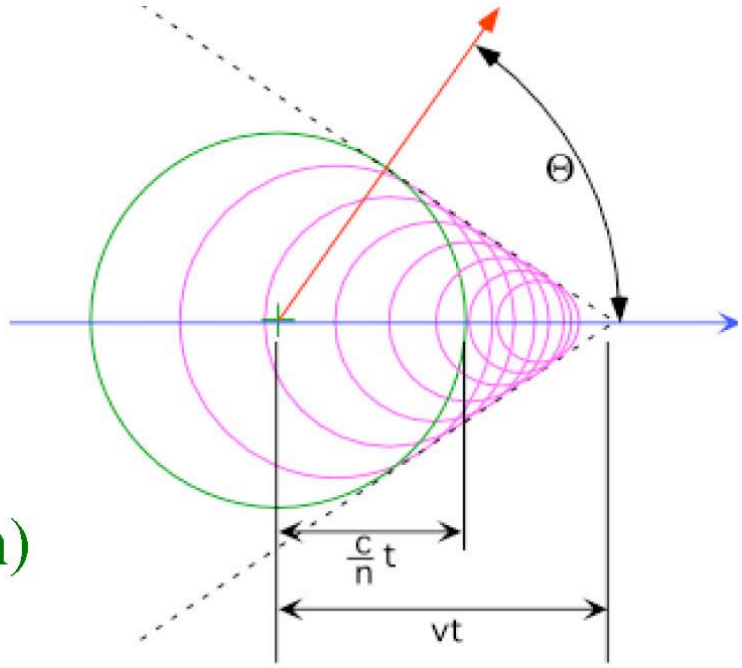


- *The number of photons emitted per cm is proportional to* $\lambda^{-2}$ $\longrightarrow$ *UV light dominates*

# *Calorimetry: Homogeneous calorimeters*

- *High-density crystals used as electromagnetic calorimeters*
  *Example: CMS ECAL, $PbWO_4$. Density 8.3 g/cm$^3$, radiation length 8.9 mm.*
- *Very good energy resolution*
- *Very expensive*
- *Radiation damage a problem*
- *Other crystals:*
  *NaI(Tl), CsI, BGO, $BaF_2$*

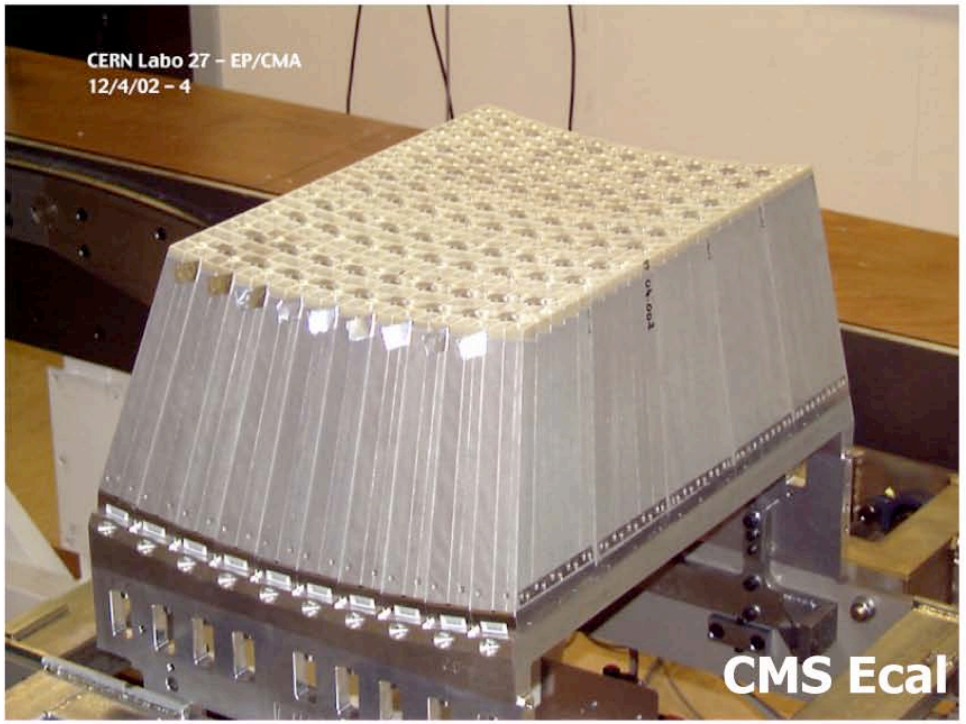

# *Calorimetry: Sampling calorimeters*

- *Different absorber and detector materials*
- *Better segmentation, energy resolution worse*
- *Absorber media: Fe, Cu, Pb, U, W*
- *Active media: Scintillator, LAr, gas…*

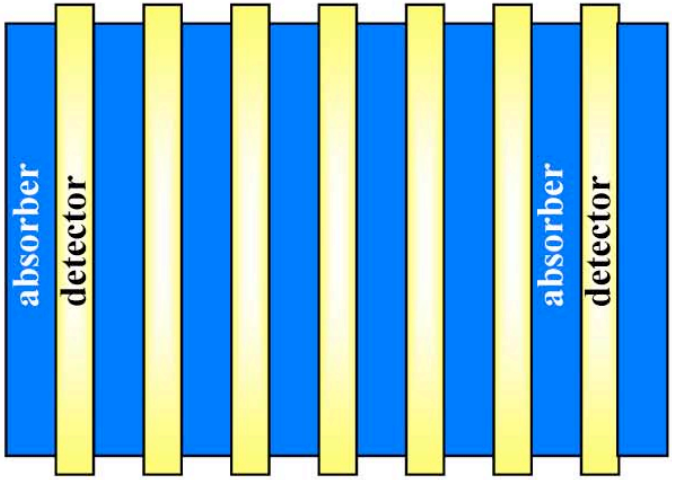


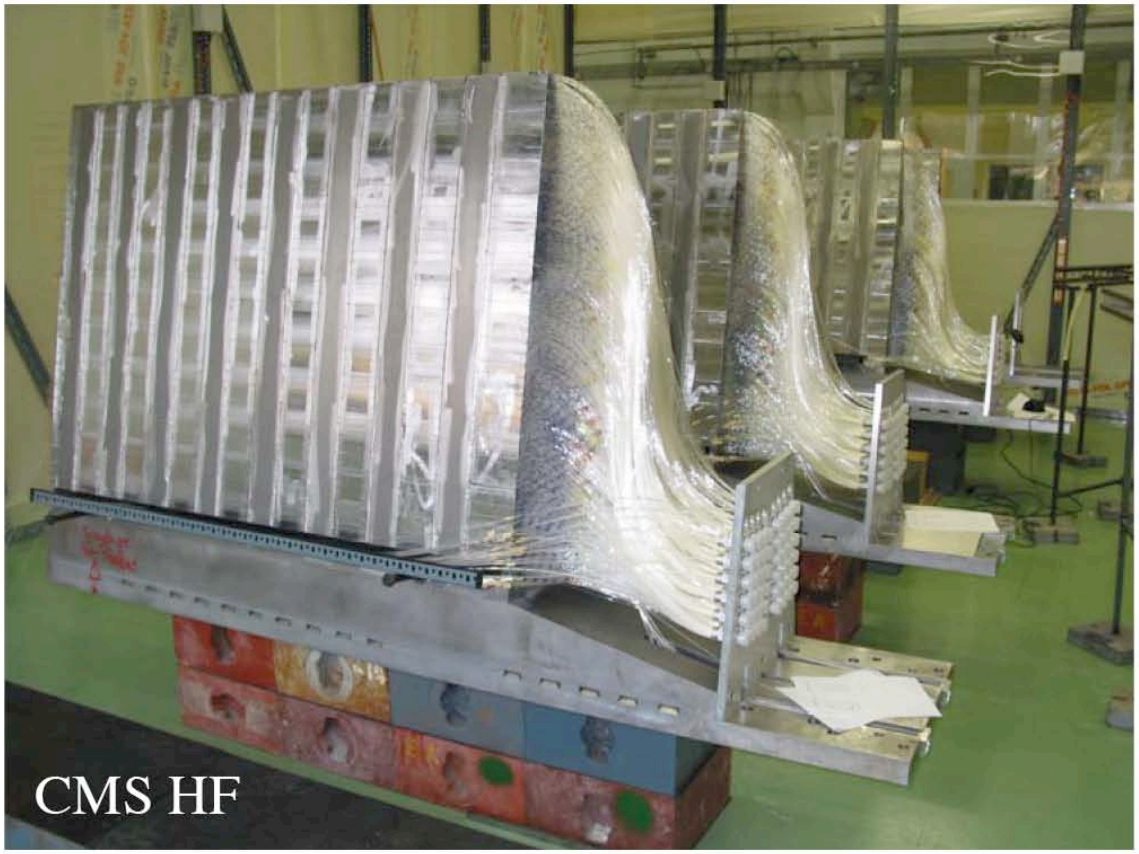


# *Scintillation detectors ("scintillators")*

- *Many materials emit light when traversed by ionizing particles*
  *Scintillation caused by excited molecules falling back to ground state*
- *Scintillation counters most widely used particle detectors*
  *(Rutherford used ZnS)*
- *Impurities often play crucial role*

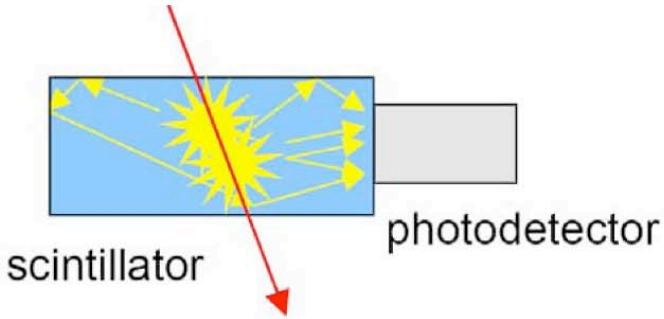


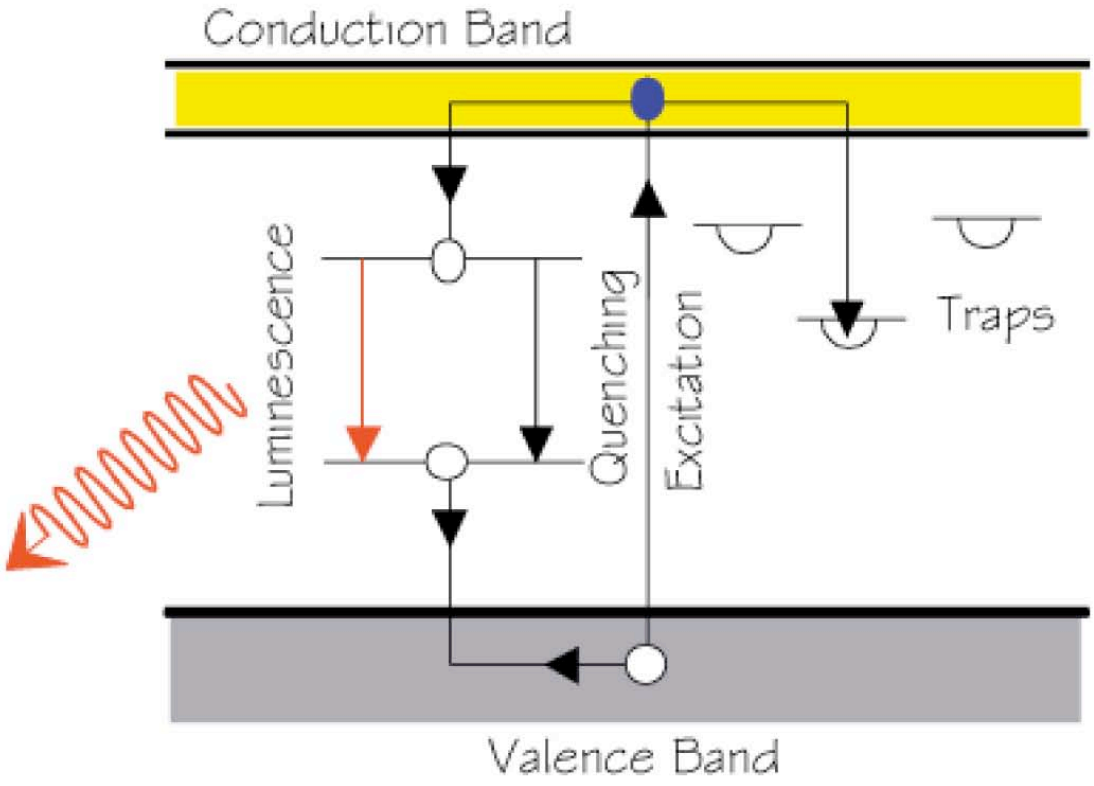


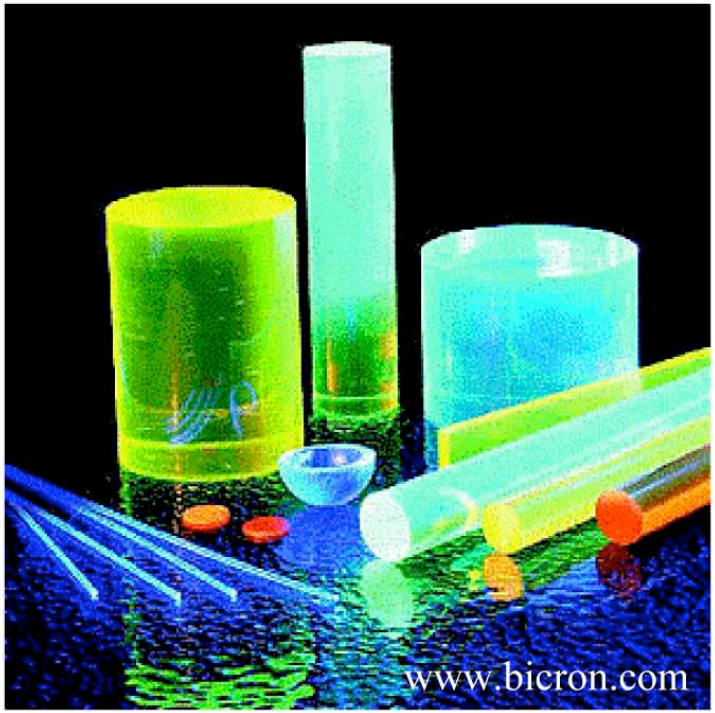

# *Scintillator types*

- *Organic: liquid, plastic*
  - Up to 10,000 photons per MeV
  - Low Z, ρ~1gr/cm$^3$
  - Doped, large choice of emission wavelength
  - ns decay times
  - relatively inexpensive
  - Easy to manufacture in any shape or size,
  - The scintillation process is a function of a single molecular process and is independent of the physical state of the scintillator

- *Inorganic: crystals*
  - High light yield, up to 40,000 photons per MeV
  - High Z, large variety of Z and ρ
  - Undoped and doped
  - ns to μs decay times
  - Expensive
  - Difficult to grow crystals
  - Require a crystal lattice to scintillate

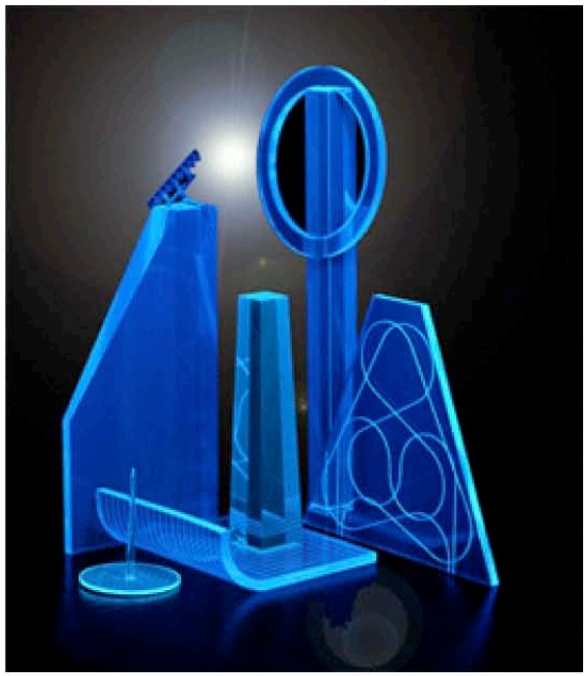

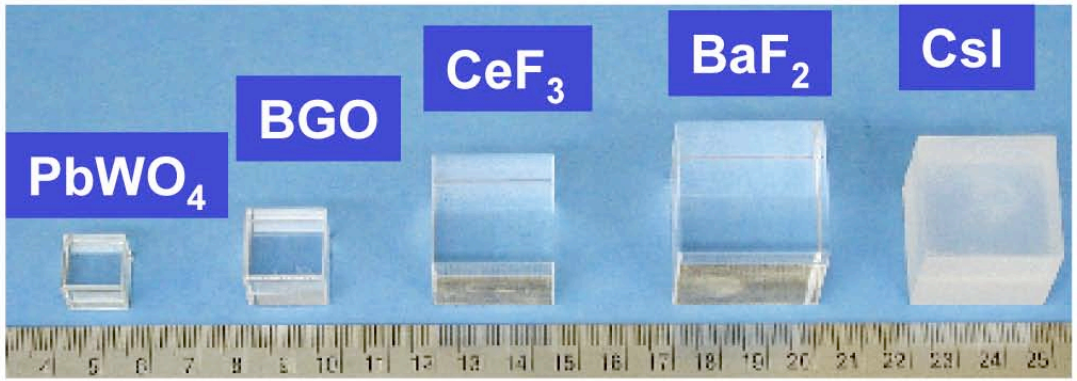


- *Wide range of applications*
- *Match emission wavelengths to detection device*

# *Light guides and Wavelength shifters*

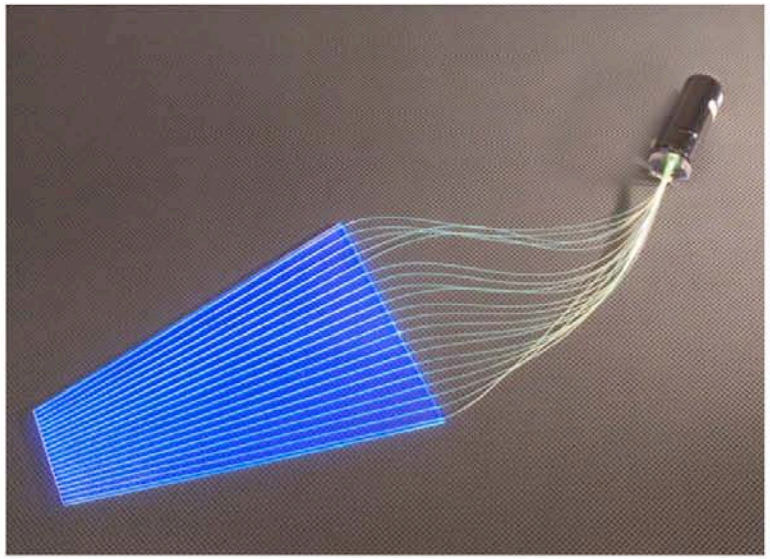

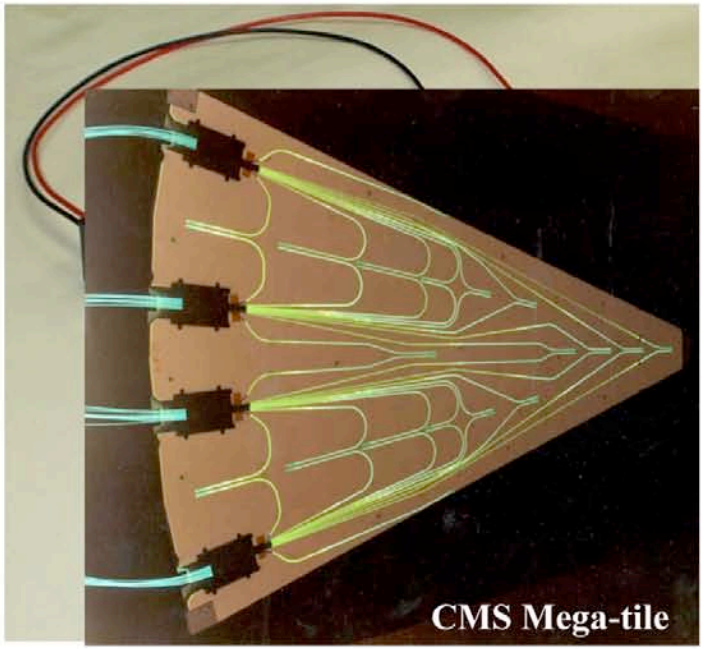


*Scintillation light absorbed and re-emitted at longer wavelength.*

*Fibers transport light through total internal reflection*

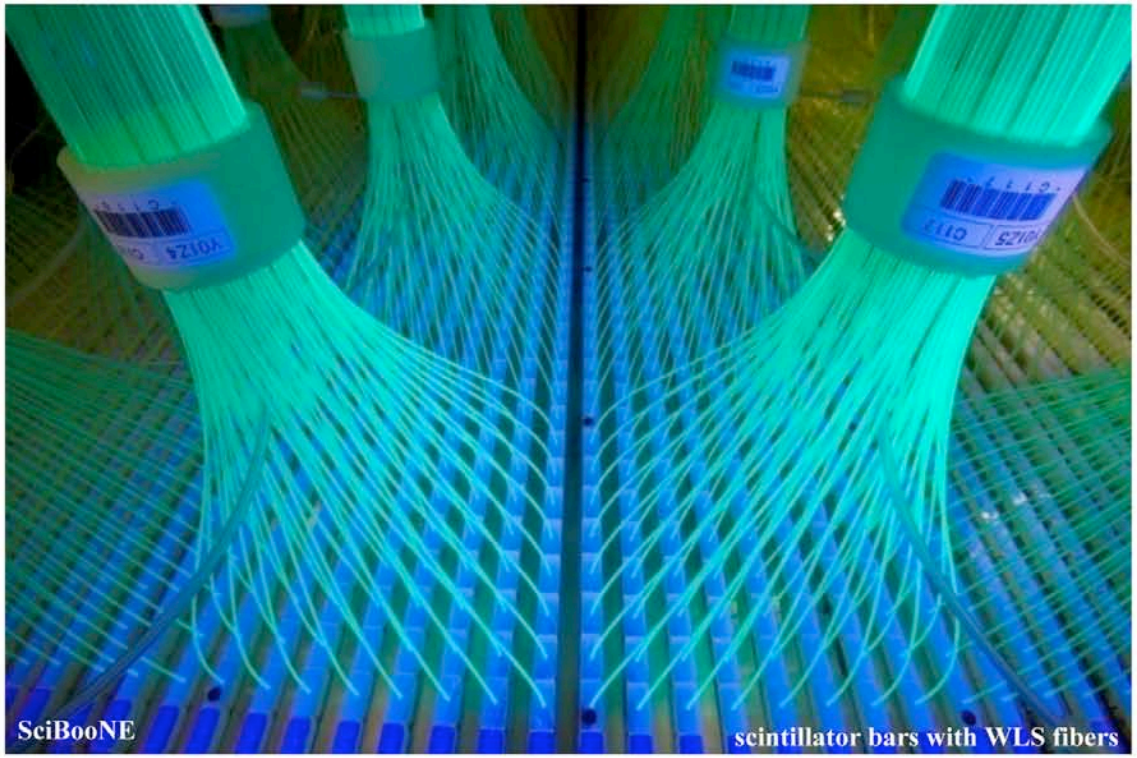

# *Scintillator use in particle physics experiments*

- *Many different shapes:*
  - *paddles, sheets, strips, blocks, fibers….*

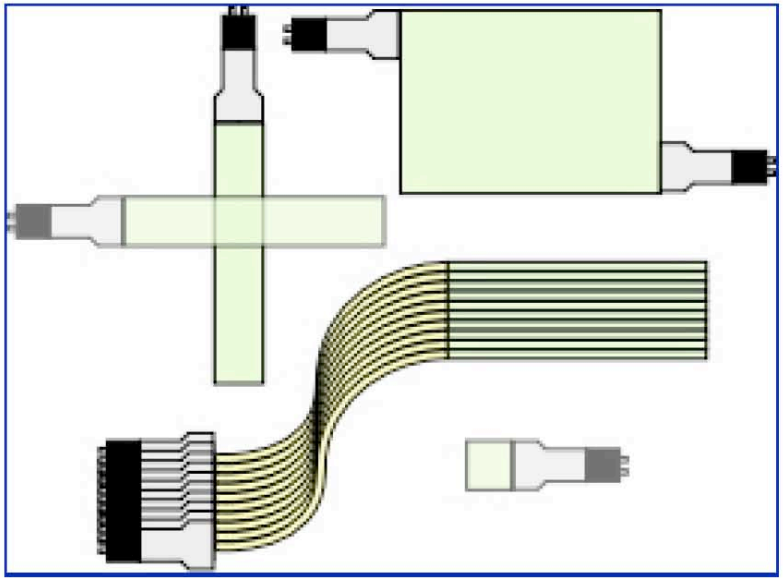

## *Used for:*

- *Timing (signals are fast)*
- *Triggering (same reason)*
- *Particle tracking*
- *Particle identification*
- *Calorimetry*

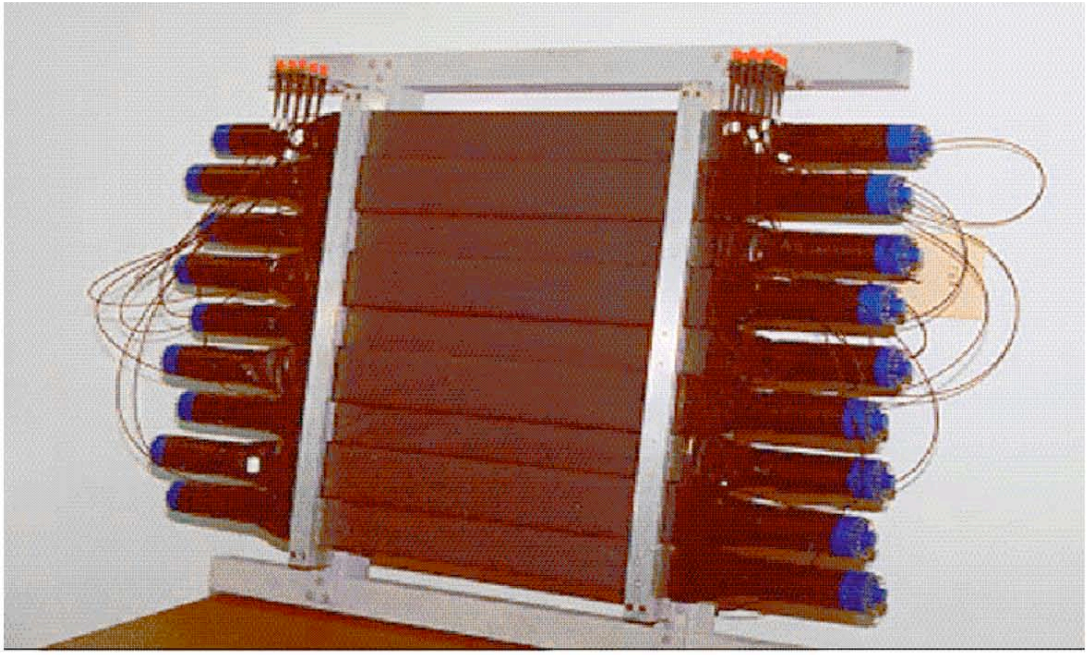

*Hodoscope*

# *Photodetectors*

- *Photocathode + secondary emission multiplication*
  - *PMT*
  - *Multichannel PMT*
  - *Microchannel plates*
- *Solid-state devices*
  - *Photodiodes (no gain)*
  - *Avalanche photodiodes (gain 10 - 100)*
  - *Solid-state photomultipliers (SiPM)*
  - *Visible light photon counters (VLPC)*

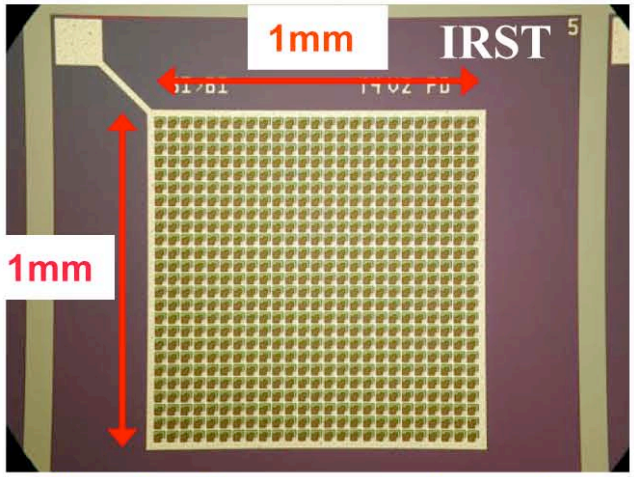


*Si pixels operating in Geiger mode*

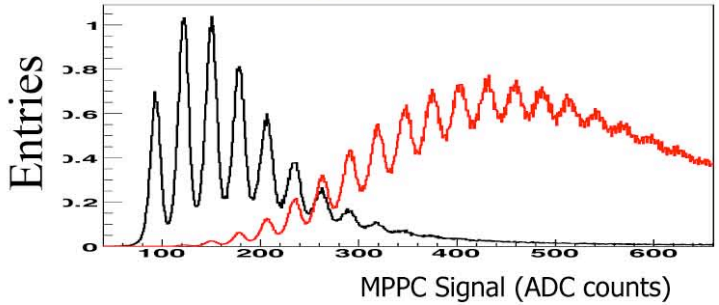


- *Hybrids: photocathode + electron acceleration + silicon*

# *Operating modes of Wire Chambers*

- **Recombination mode**
  - No charge collection
- **Ionization mode**
  - Full charge collection, but no charge multiplication; gain ~ 1
- **Proportional mode**
  - Multiplication of ionization; detected signal proportional to original ionization → possible energy measurement (dE/dx); secondary avalanches have to be quenched; gain ~ $10^4$ – $10^5$
- **Limited proport. mode (saturated, streamer)**
  - Strong photoemission; secondary avalanches merging with original avalanche; requires strong quenchers or pulsed HV; large signals → simple electronics; gain ~ $10^{10}$
- **Geiger mode**
  - Massive photoemission; discharge stopped by HV cut; strong quenchers needed as well

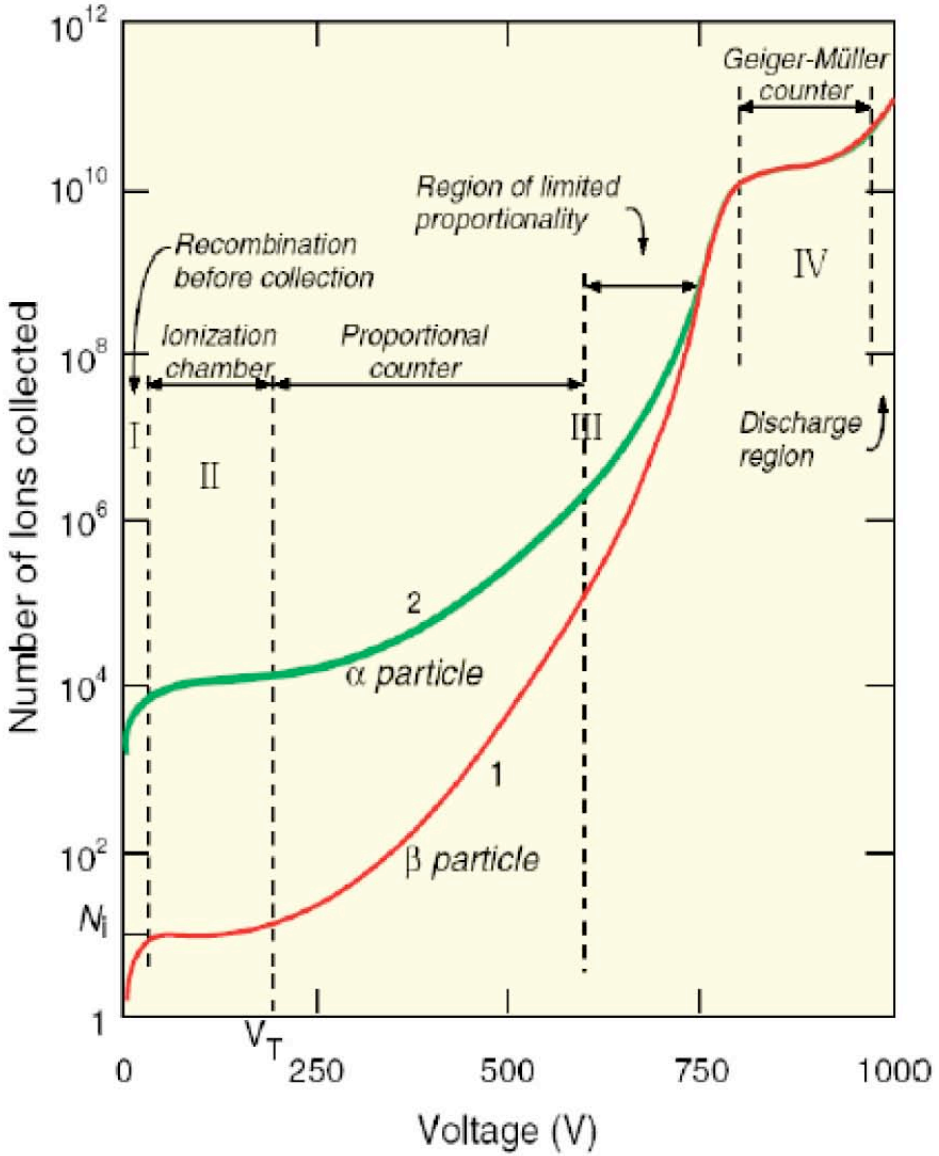

# *Non-gaseous Ionization Detectors*

## *("Ionization Chambers")*

*Dense material* → *lots of charge. Typically no charge amplification.*

- *Semiconductors* → *Silicon (strips, pixels), GaAs, Diamond*
- *Noble liquids* → *Liquid argon, krypton, xenon*

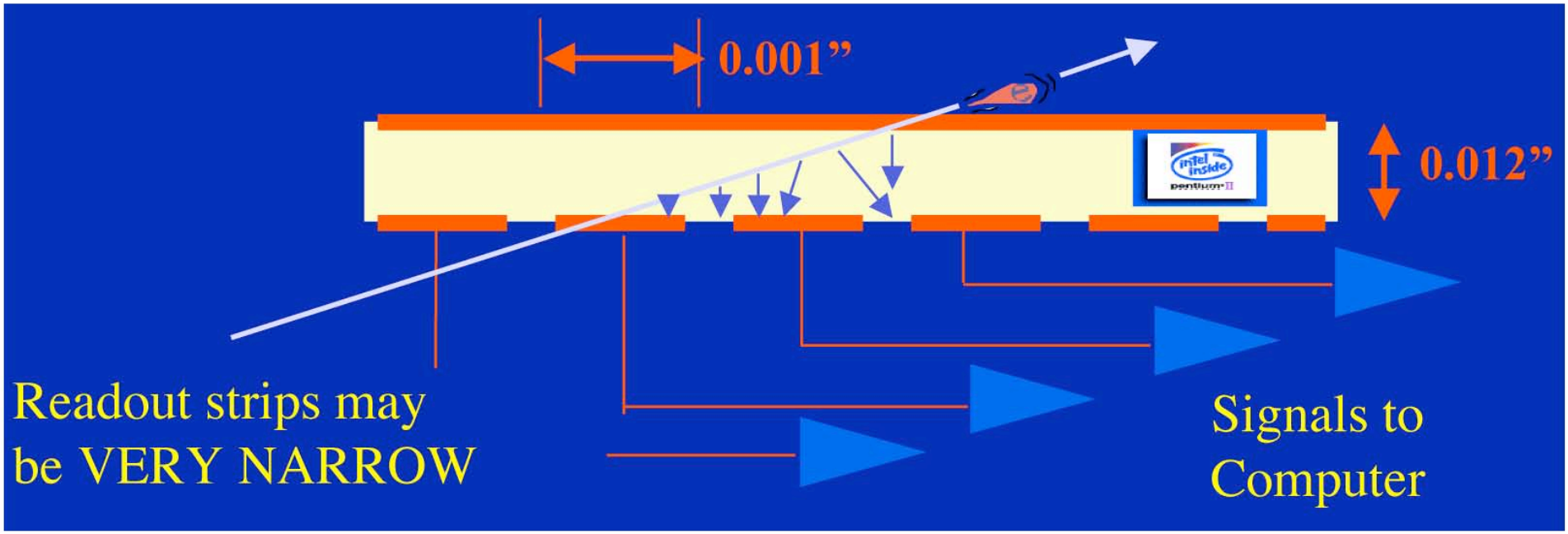

# *Directionality of Čerenkov light can be applied in calorimeters*

- *Čerenkov* light is emitted by *relativistic charged* particles ($\beta > 1/n$)
  *e.g.* quartz ($n = 1.45$): Threshold 0.2 MeV for $e$, 400 MeV for $p$

  Light is emitted at angle $\theta = \arccos(\beta n)^{-1}$ ($\sim 45^\circ$ for $\beta \sim 1$ in quartz)

- *Optical fibers* only trap light emitted within the *numerical aperture*

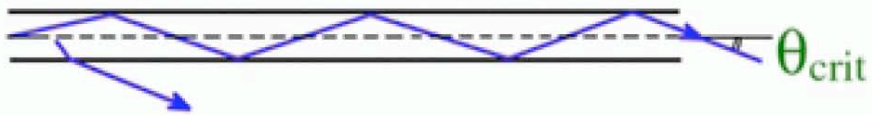


$\theta_{crit} \sim 20^\circ$ for quartz fibers

- Comparison of *Čerenkov* light (directional) and *scintillation* light (isotropic) produced in fiber calorimeters is a rich source of information on details of shower development

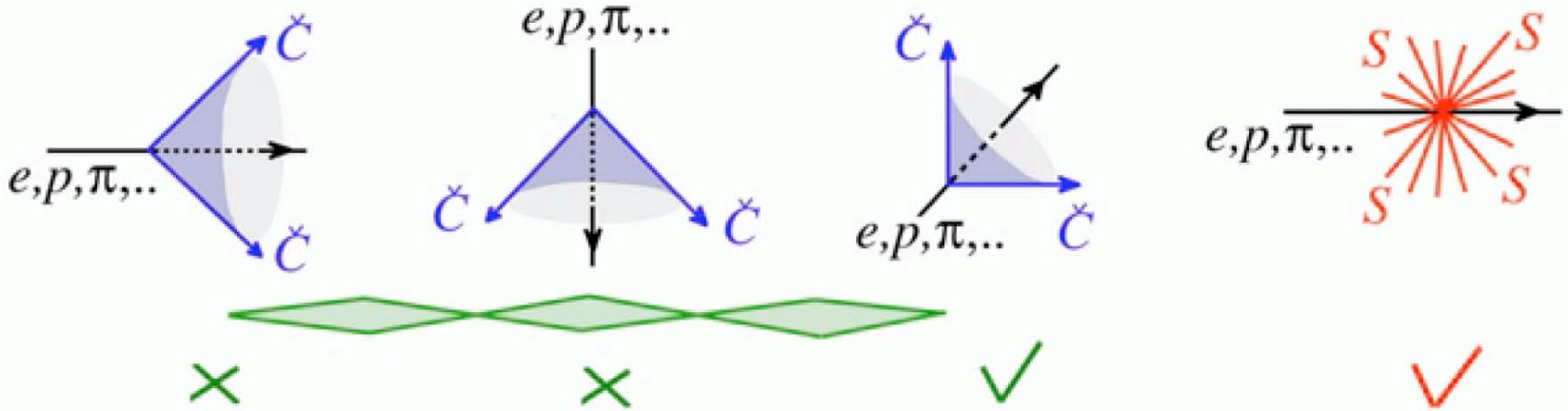

# The changing angular distribution of shower particles

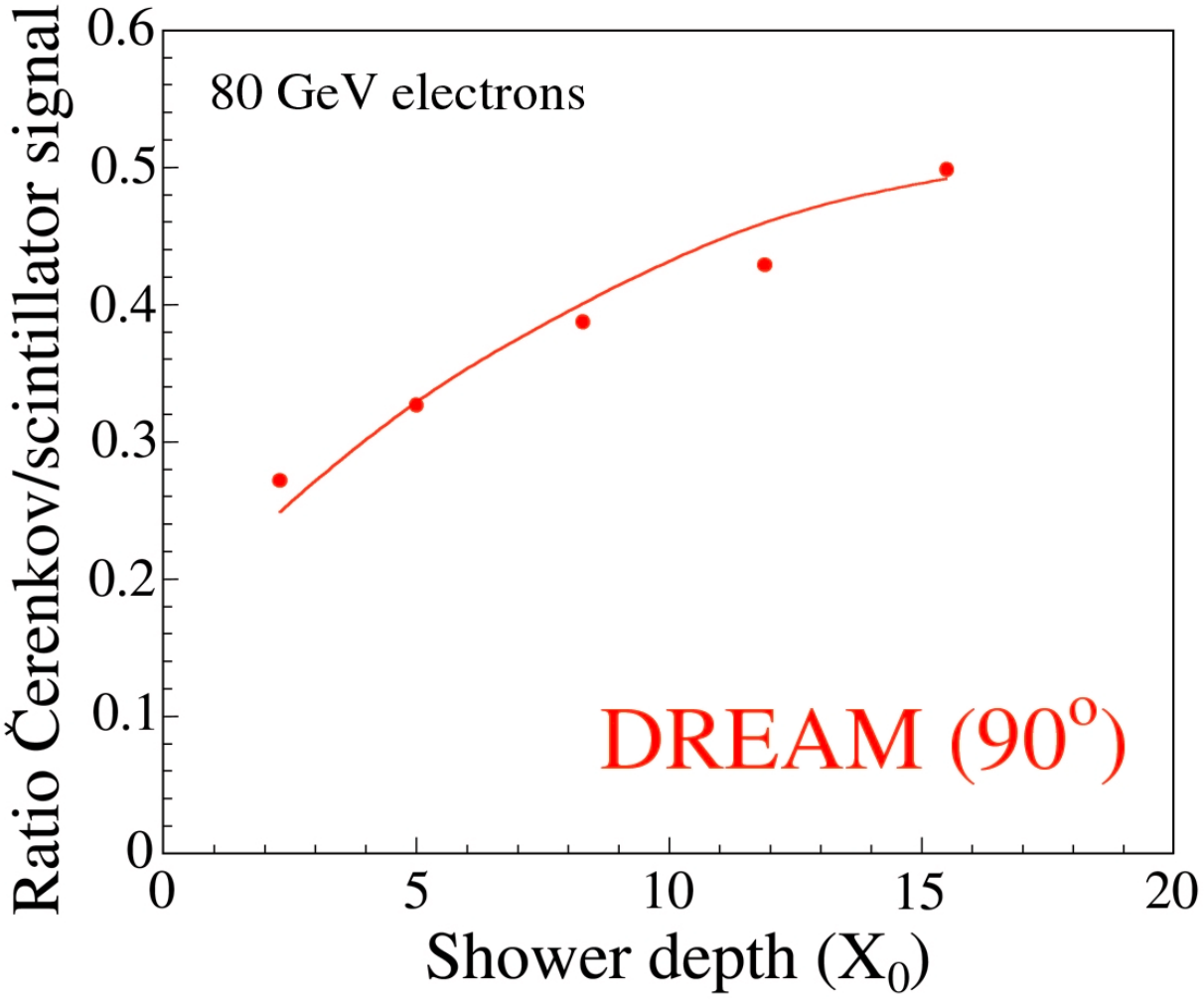

# *Calorimetric separation of ionization / radiation losses*

## Muon signals in the DREAM calorimeter

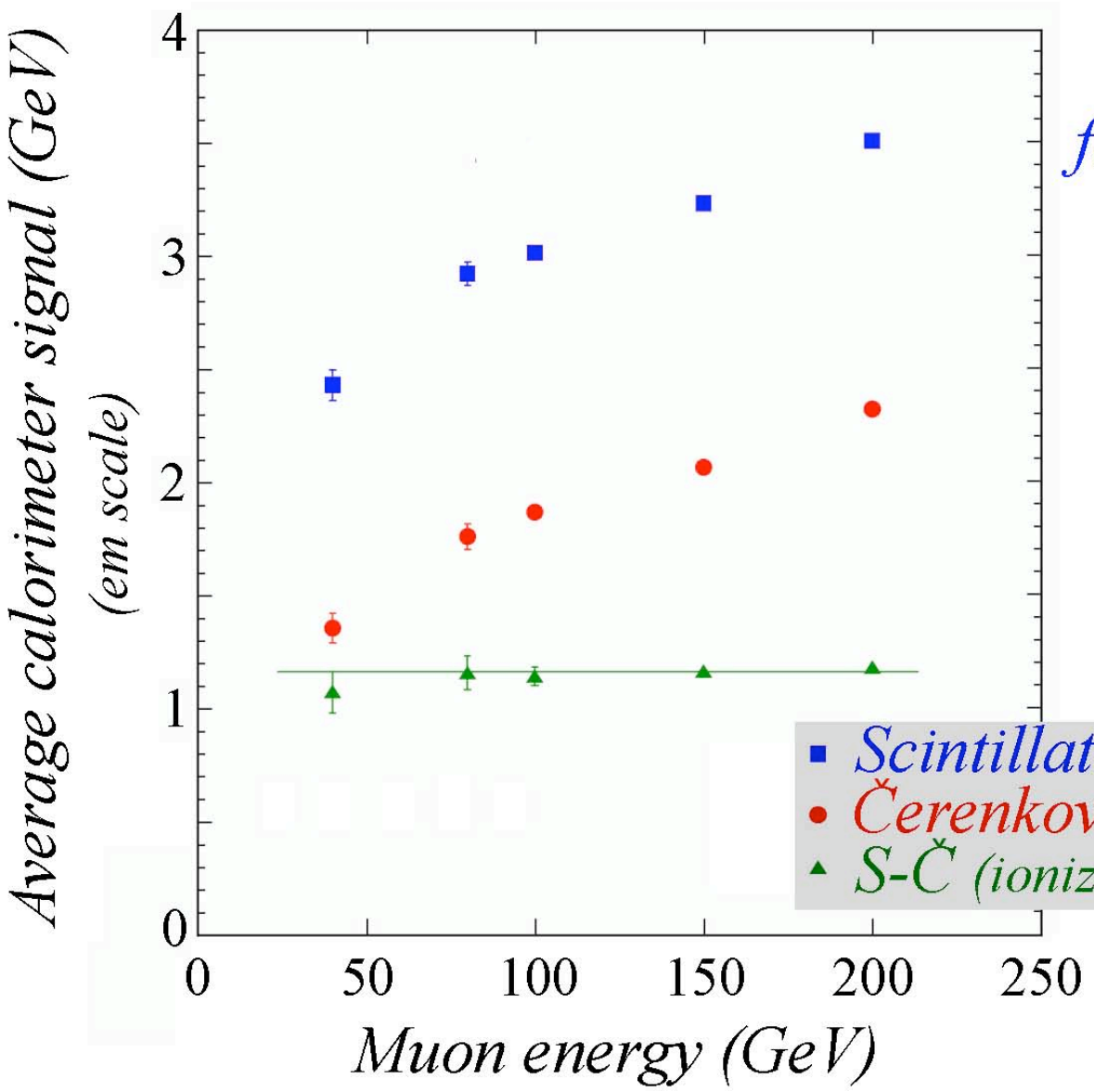


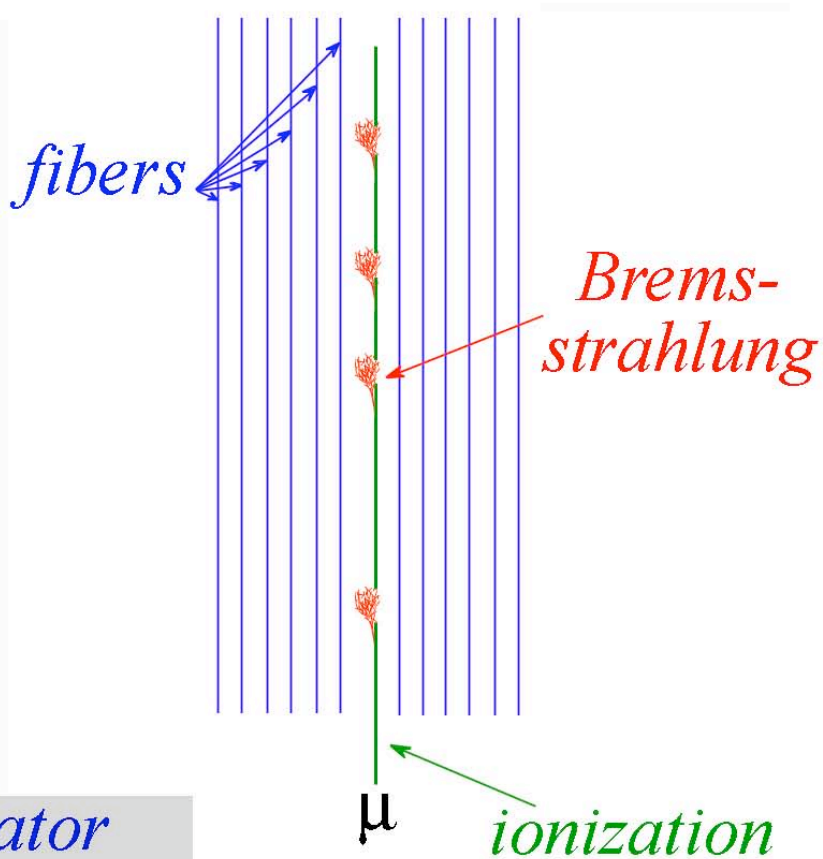


*From:* NIM A533 (2004)305

# *Particle ID with calorimeters*

# Calorimeters

## Electromagnetic shower development

*Processes that play a role in total absorption of high-energy particles are more complicated than just ionization of the traversed material*

- *Electrons: "bremsstrahlung". Photons: Compton effect, pair production*
  - Radiation of real photons in the Coulomb field of the nuclei of the medium
    - Any deflection of the electron from its original trajectory accompanied by radiation of photons and deceleration of electrons

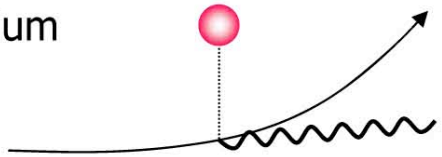

  - Photo-electric effect

$$\sigma_{ph-el} \propto Z^5 \frac{1}{\varepsilon} \qquad \varepsilon = \frac{E_\gamma}{m_e c^2}$$

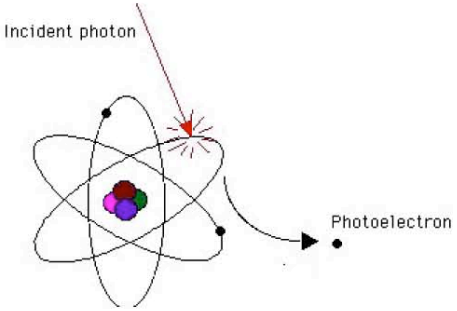


  - Compton scattering: $\gamma + e \rightarrow \gamma' + e'$

$$\sigma_c \propto \frac{\ln \varepsilon}{\varepsilon}$$

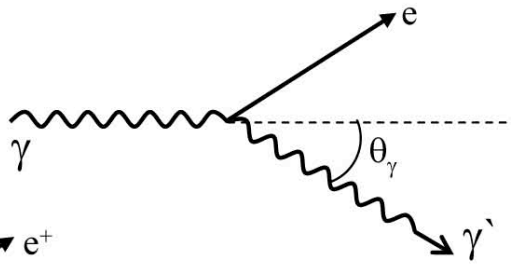


  - Pair production: $\gamma$ + nucleus $\rightarrow e^+ e^-$ + nucleus
    - Process independent of energy
    - Dominates at high energies

$$\sigma_{pair} \propto Z^2$$

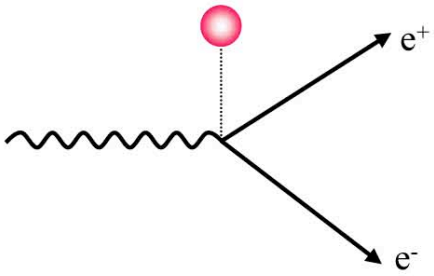

# *Calorimeters*

## *Electromagnetic shower development*

*When a high-energy electron or photon enters a calorimeter, its energy is absorbed in a cascade of processes in which many different "shower" particles are produced.*

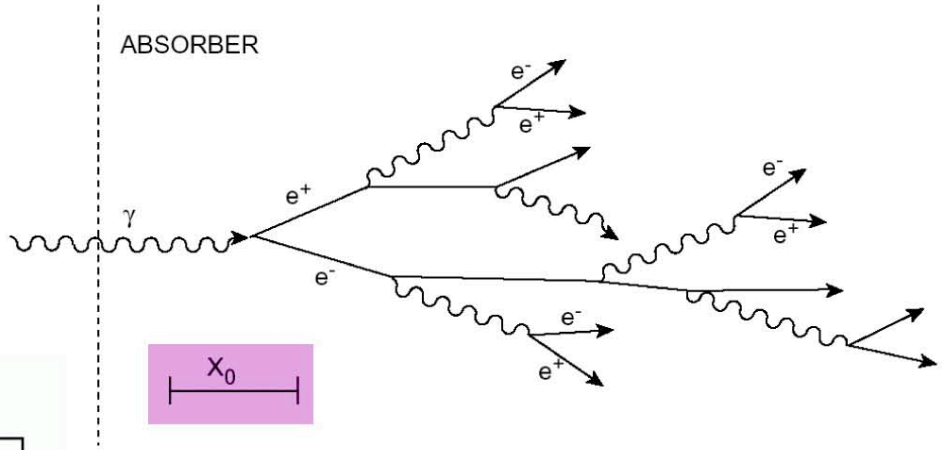


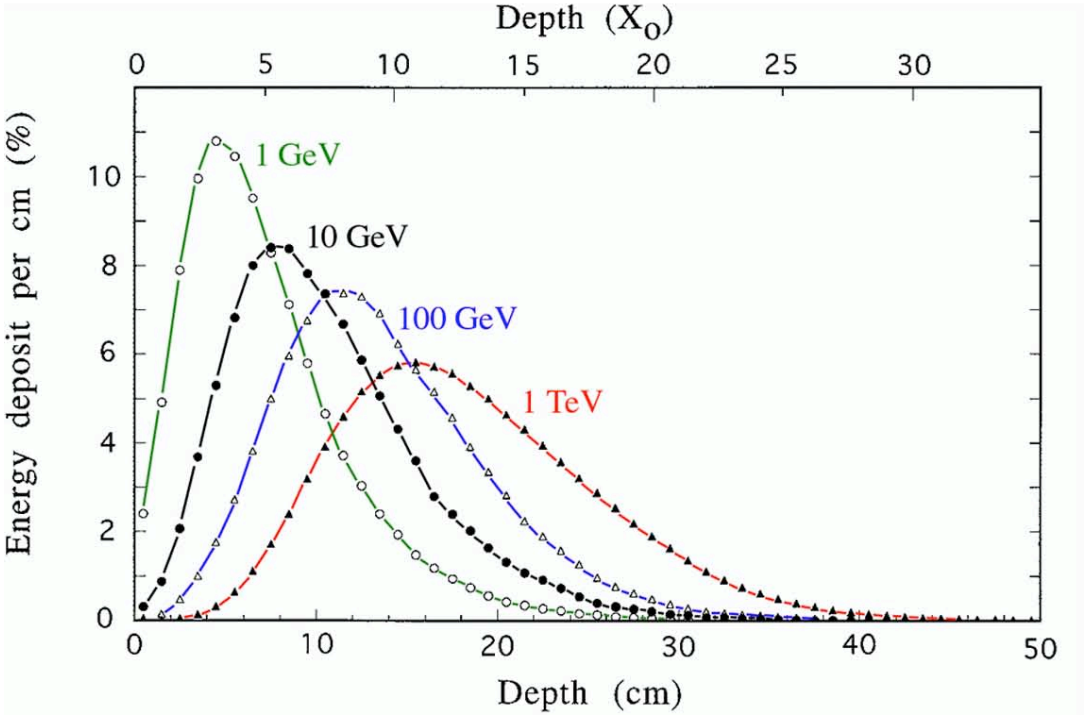


*The shower development is governed by the "radiation length" $X_o$, which is typically ~ 1 cm*

*Even very-high-energy particles are absorbed in relatively small detectors (99% of 100 GeV $e^-$ in 10 kg)*

# Calorimeters

## Hadronic shower development

- *There are many more processes involved in hadronic shower development. Also, some fraction of the energy is deposited through electromagnetic cascades*
- *A hadronic shower consists of two components*
  - *Electromagnetic component*
    - electrons, photons
    - neutral pions → 2 γ
  - *Hadronic (non-em) component*
    - charged hadrons $\pi^{\pm}$,$K^{\pm}$
    - nuclear fragments, p
    - neutrons, neutrino's, soft γ's
    - break-up of nuclei *("invisible")*

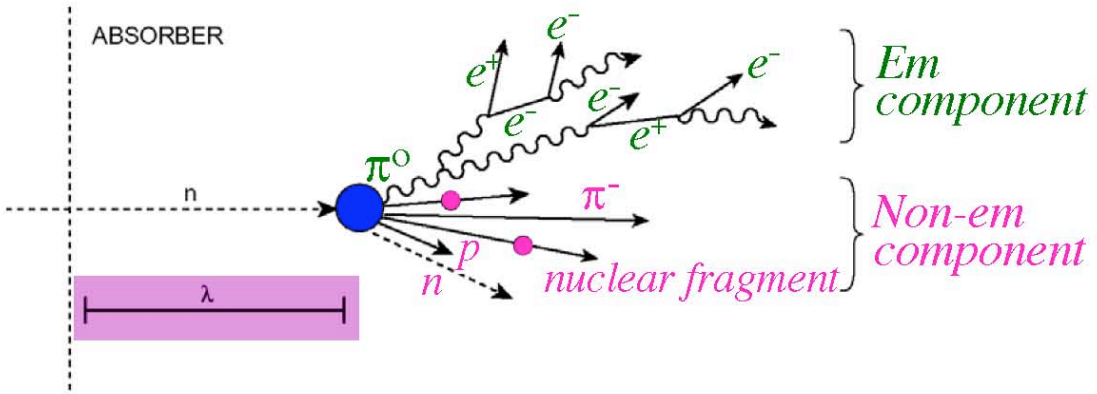


- *Hadronic shower development governed by nuclear interaction length λ*
  *λ is typically $\gg X_0$, ~20 cm → it takes tonnes to contain hadronic showers*
- *Hadronic showers are characterized by very large fluctuations*
- *Calorimetric techniques are destructive, but work for charged + neutral particles*

# *Average (!) hadronic shower profile (longitudinal)*

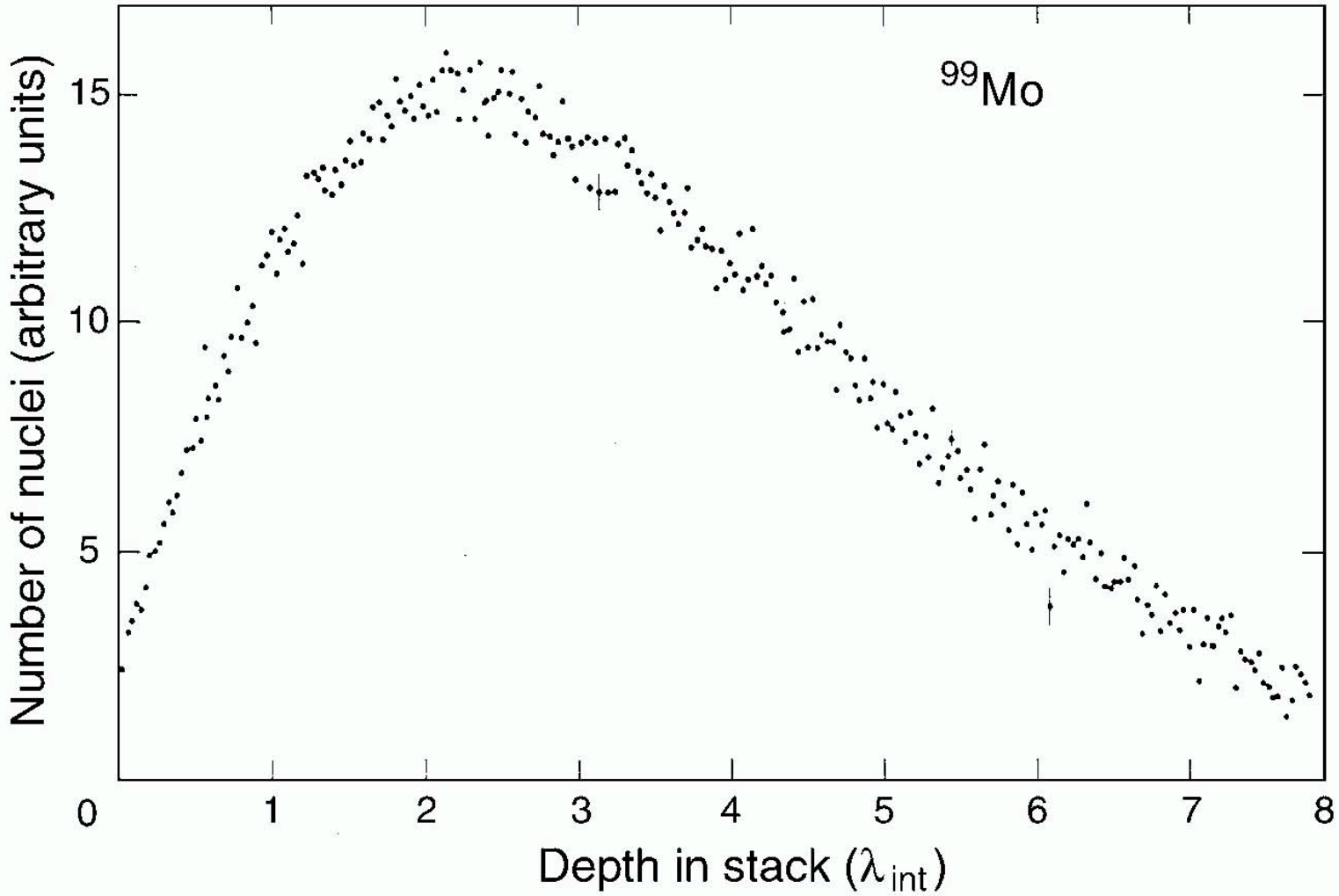


FIG. 2.31. Longitudinal shower profile for 300 GeV $\pi^-$ interactions in a block of uranium, measured from the induced radioactivity. The ordinate indicates the number of radioactive decays of a particular nuclide, $^{99}$Mo, produced in the absorption of the high-energy pions. Data from [Ler 86].

# Comparison of em / hadronic calorimeter properties

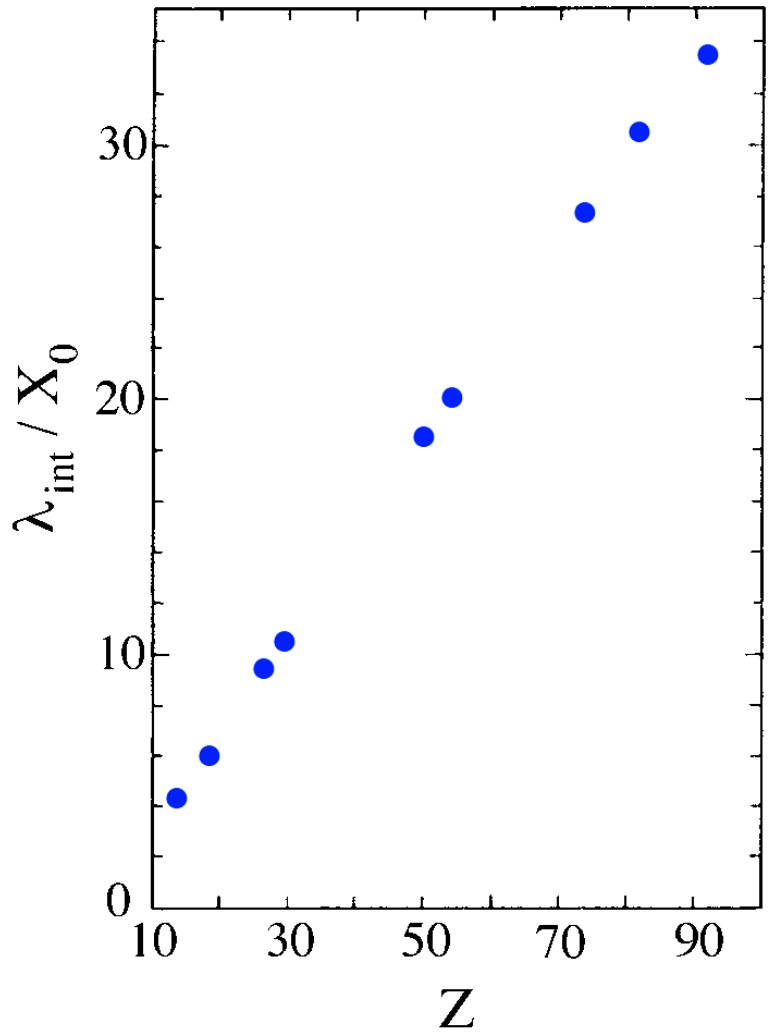


FIG. 7.28. Ratio of the nuclear interaction length and the radiation length as a function of $Z$.

# Particle ID with a very simple Preshower Detector

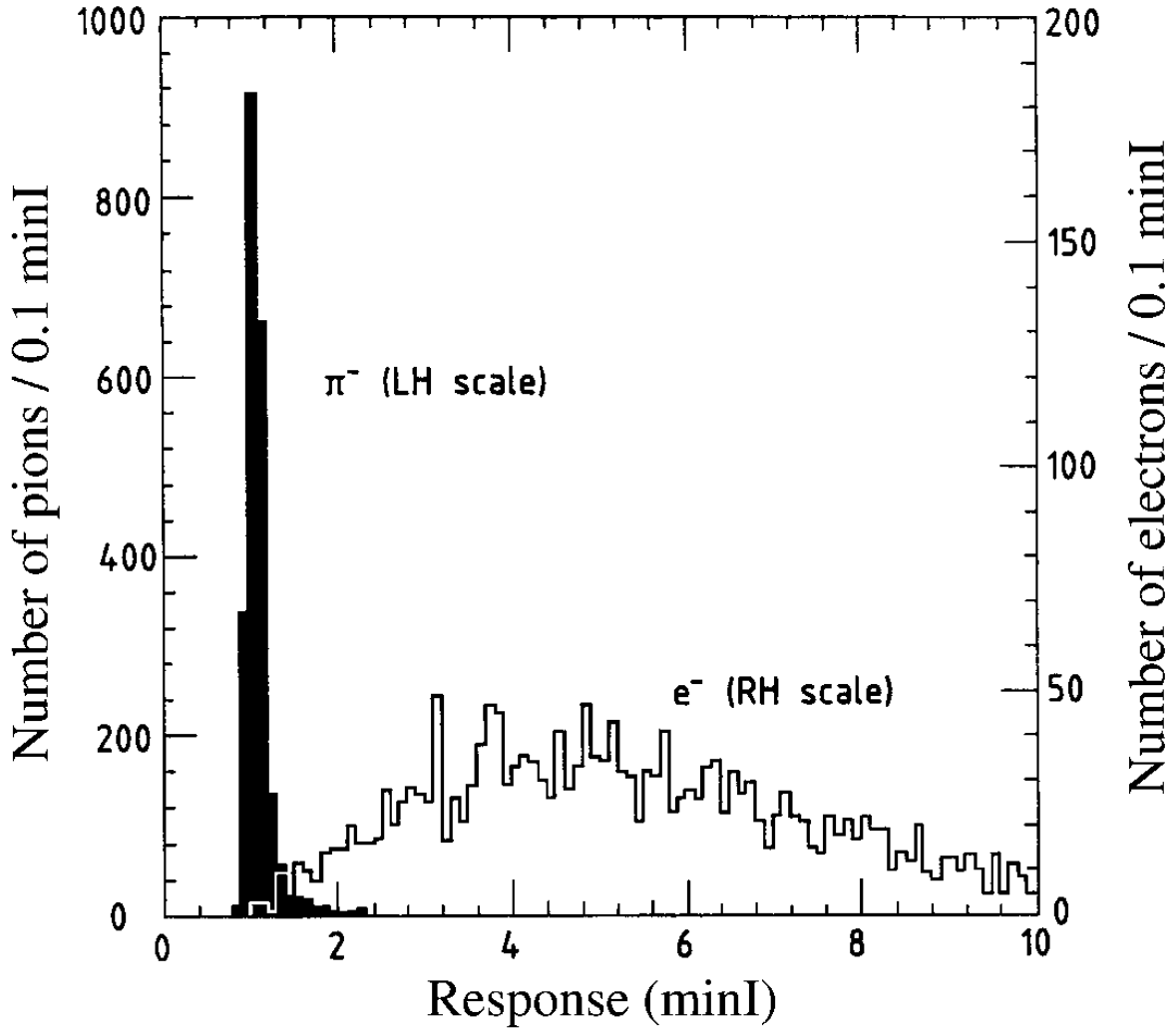


FIG. 7.35. Signal distributions for 75 GeV pions and electrons in a preshower detector used in beam tests of CDF calorimeters.

# *Particle identification with calorimeters*

## e/π separation using time structure signals

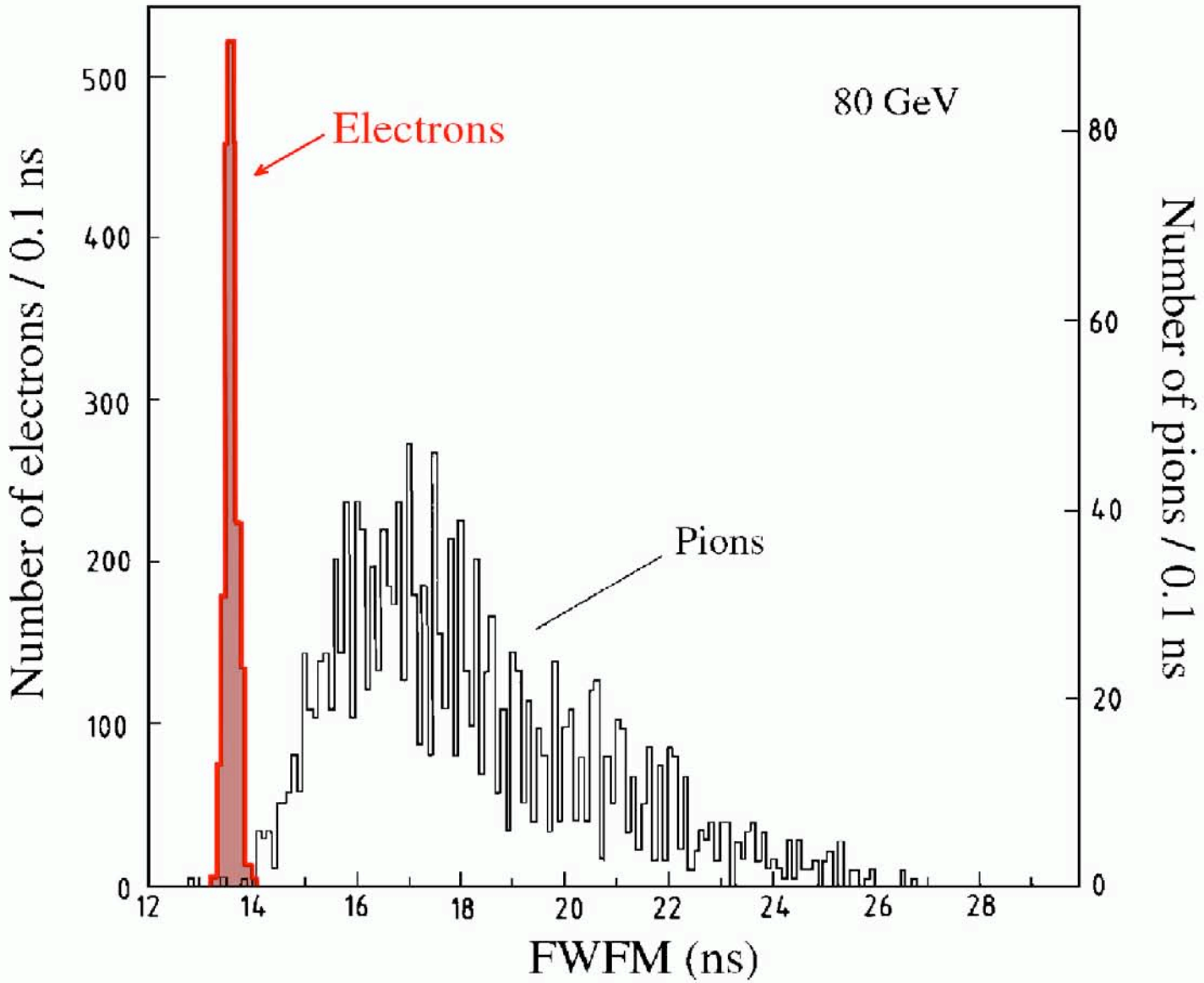


FIG. 7.33. The distribution of the full width at one-fifth maximum (FWFM) for 80 GeV electron and pion signals in SPACAL [Aco 91a].

# *The jet energy scale*

## *How to get there?*

# *Calibration: from photons to GeVs*

*This is a multi-step process.*
*We will use the ATLAS TileCAL as an example*

- *The readout system of the ATLAS TileCAL consists of 9852 PMTs*
  *These convert photons into electric signals (charge, measured in pC)*

- *First, these PMTs need to operate in a stable way.*
  *A change of 50 V in the operating voltage gives a factor 2 change in gain*
  *Monitor gain stability by injecting laser light in each PMT*

- *The light is produced inside the tiles and transported to the PMTs with wavelngth shifting fibers*

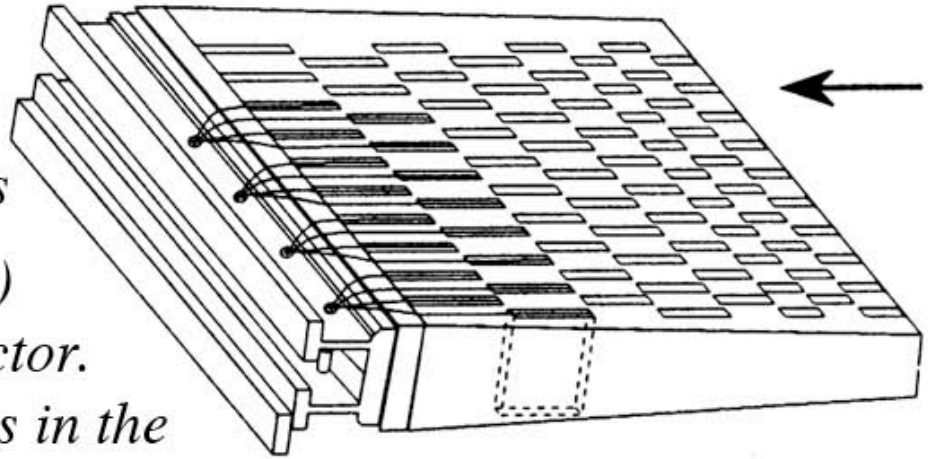

- *Move a radioactive source ($^{137}Cs$) in the z direction through the detector.*
  *Individual tiles are visible as peaks in the current measured by the PMTs*
  *Equalize the signals in the various PMTs by means of the high voltage*

→ *The same energy deposit leads to the same signal (in pC) anywhere in the detector*

# *Calibration: from photons to GeVs (2)*

- *Problem: The range of the γs emitted by the source is very limited (~ 1 cm)*
  *The source thus probes only a small region of each calorimeter tile*
  *A separate effort is needed to check/achieve that the signal does not vary (much) over the surface of the tile.*
  *N.B. This may change over time (radiation damage, chemical ageing)*
  *One hopes/expects to recognize/monitor such effects from regular source scans*

- *The next step is relate the picoCoulombs measured by the PMTs to the shower energy, measured in GeVs. This is done by exposing (a fraction of) the detector modules to beam particles of known energy. Typically one uses electrons for this purpose, since these particles deposit all their energy in a limited region, covered by one or a small number of PMTs*
  *This gives calibration constants, in pC/GeV*

- *Finally, the TileCal modules are placed behind a module of the LAr ECAL, and exposed to beams of pions of different energies*
  *If one uses the calibration constants determined above, one finds that the energies of these pions are systematically measured too low, more so if the beam energy is lower. This is a consequence of the non-compensating nature of the calorimeters*

# *Calibration: from photons to GeVs (3)*

- *In a final step, called "off-line compensation", a complicated correction procedure is applied in which the calibration constants are modified so that the pion energies are reproduced.*
  *Is is not clear at all that this method would also give meaningful results for jets, which are a mixture of γs (for which the original calibration constants apply) and the pions (modified constants).*

- *In any case, the proof is in the pudding.*
  *One should check to what extent this procedure reproduces a physics process such as* $Z \rightarrow b\,\bar{b}$ *correctly.*
  *This has not been done*

# *Calibration: from pC to ADC counts (0)*

*The charge produced by the PMTs is digitized by ADCs*
*The stability of this process has to be monitored as well, since the experimental information is recorded in the form of ADC counts.*

*Use the charge stored in capacitors for this purpose*

# *Calibration*

## *The pitfalls of longitudinal segmentation*

# *Calibration of longitudinally segmented devices*

- *Imagine a Cherenkov calorimeter, e.g. lead glass*
- *High-energy electrons develop showers in this*
- *On average, 10 p.e. per GeV deposited energy*
  *100 GeV e gives a signal of 1000 p.e.,*
  *10 GeV e gives a signal of 100 p.e., etc.*
- *Shower particles < 0.3 MeV give NO Č light*
- *The relative contribution of such particles increases with depth*

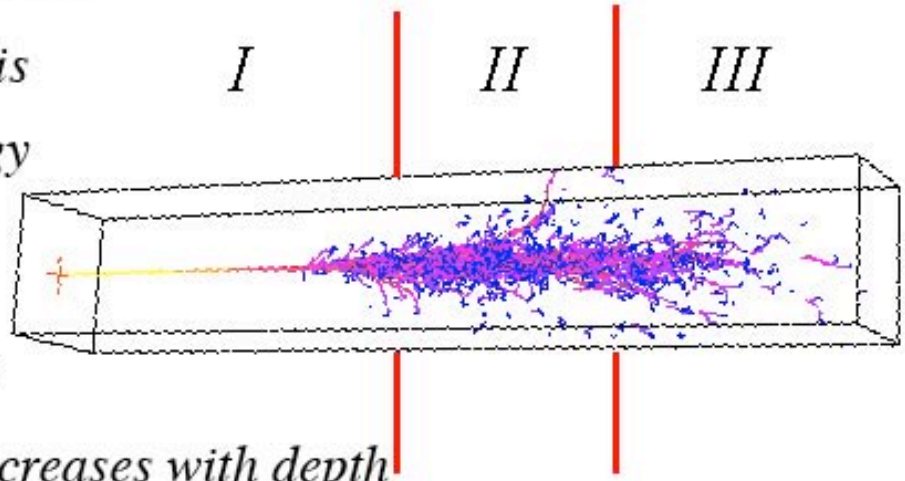


- *If this detector is cut into 3 parts, the relationship between deposited energy and resulting signal is then, e.g.*

*I: 15 p.e./GeV  II: 10 p.e./GeV  III: 5 p.e./GeV*

*These constants have been derived for 100 GeV e, which deposit, on average, 30/40/30% in these 3 parts, and thus give, on average, a signal of 1000 p.e., as before*

- *However, a low-energy shower deposits most of its energy in part I. Based on these calibration constants, its energy is OVERESTIMATED*
- *And for an em shower starting in section III (e.g. γ from $\pi^0$ decay), the energy is systematically UNDERESTIMATED*

→ *Non-linearity + energy dependence on starting point shower*

*Sampling fraction of γs, generated at random points inside a calorimeter*

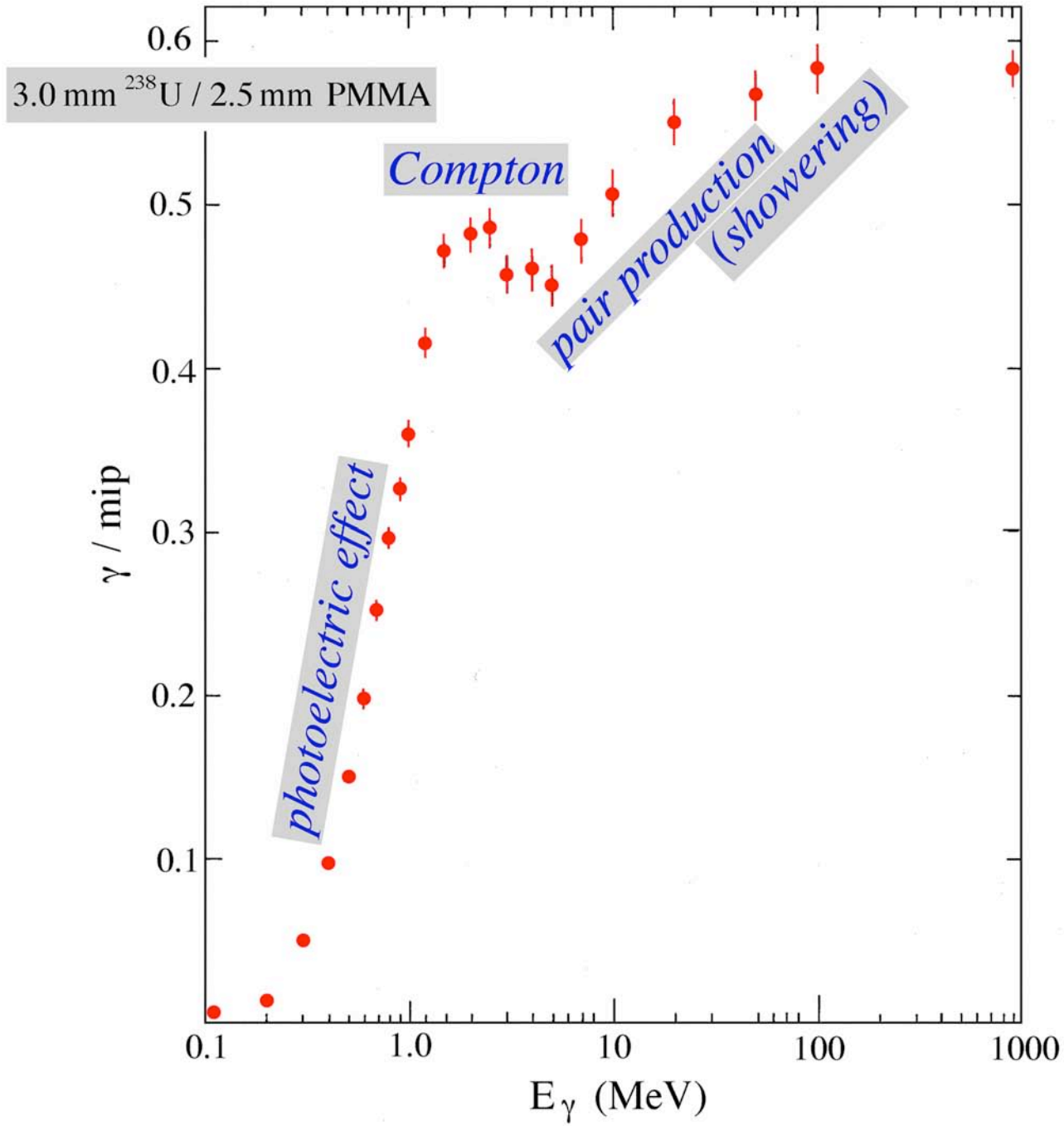

# *The sampling fraction changes as shower develops**

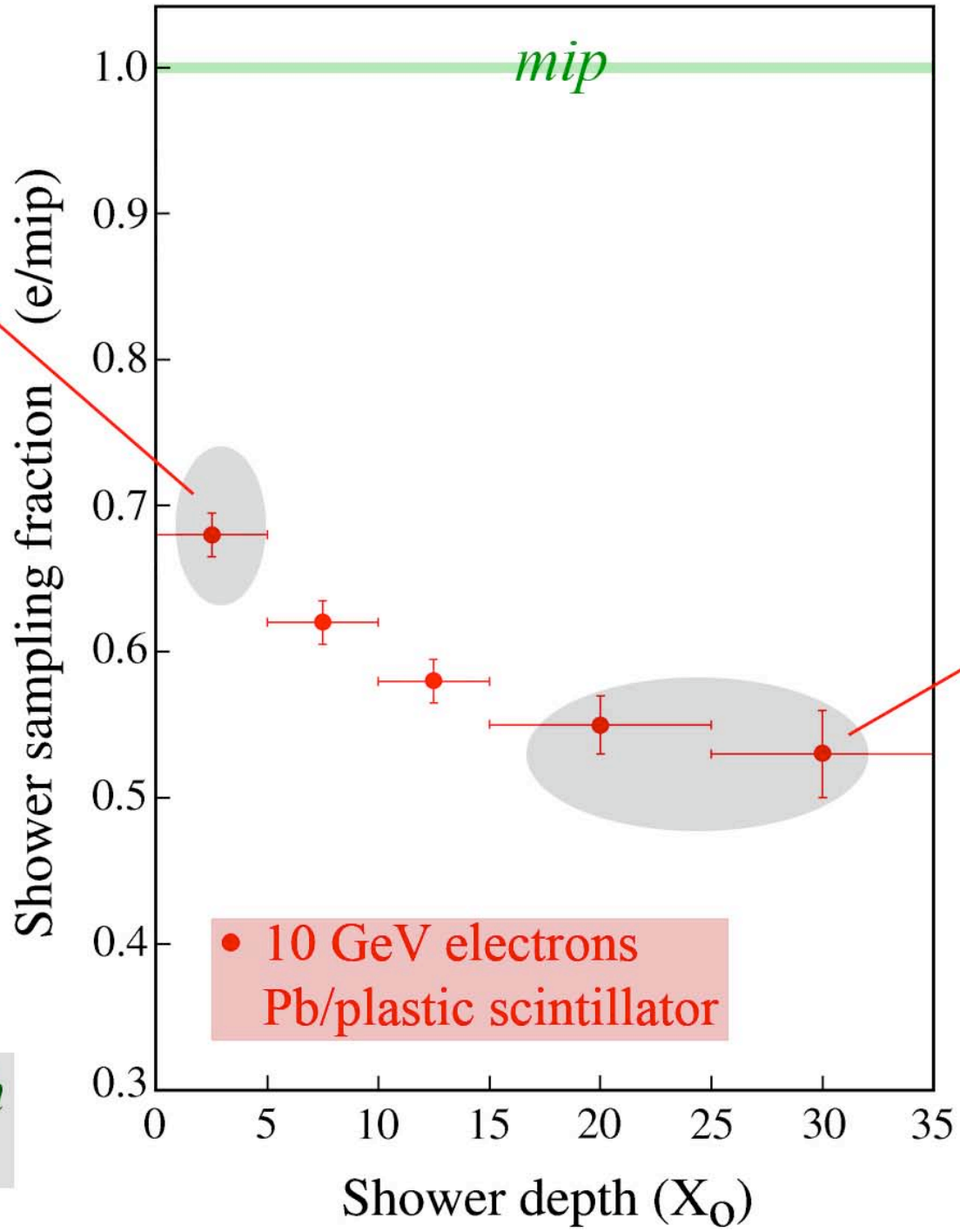


*shower dominated by mip's*

*shower dominated by soft γ's*

**By as much as 30%!*

# *Calibration misery of longitudinally segmented devices*

## *Example: AMS (em showers!)*

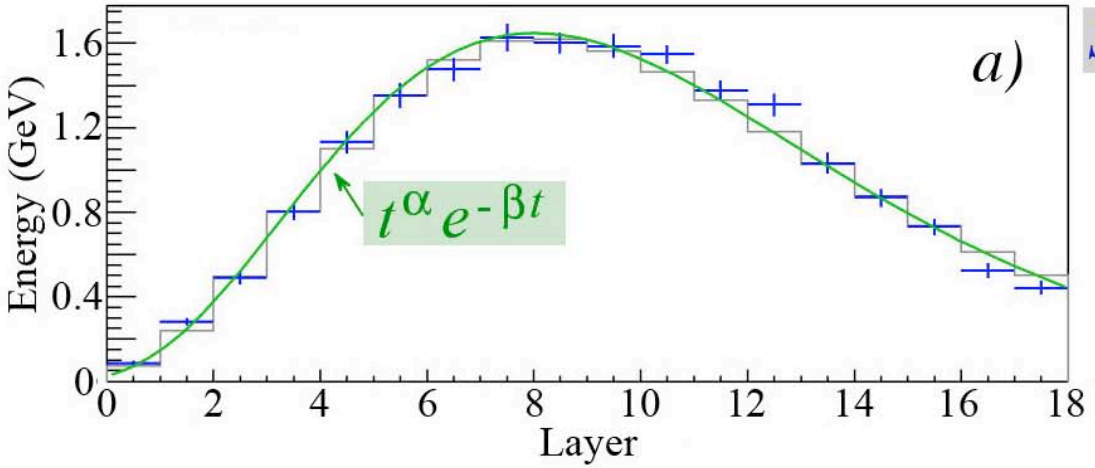


*Source: NIM A490 (2002) 132*

*Pb/scintillating fiber (18 layers)*

*Calibrated with mip's:*
*11.7 MeV/layer*

*Leakage estimated from fit to measured shower profile*

*However:*
*In em shower, signal per GeV* ***decreases*** *as shower develops*

→ *(leakage) energy based on measured signals* ***underestimates*** *reality*

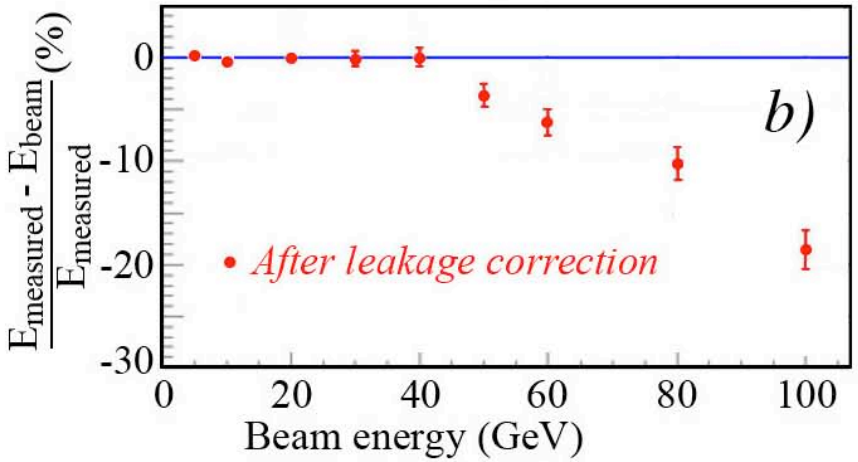


*Required very elaborate MC simulations to solve, since effects depend on energy and direction incoming particle*

*A widely used technique for calibrating segmented devices*

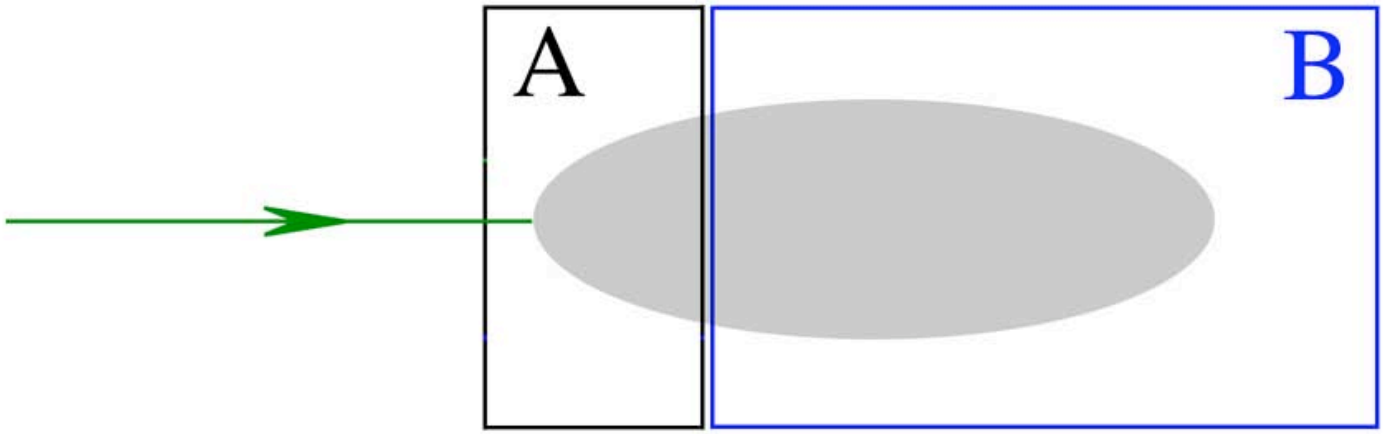


Minimize $$Q = \sum_{j=1}^{N} \left[ E - A \sum_{i=1}^{n} S_{ij}^{\mathrm{A}} - B \sum_{i=1}^{n} S_{ij}^{\mathrm{B}} \right]^2$$

→ *Determine A,B*

# Calibrating longitudinally segmented calorimeters

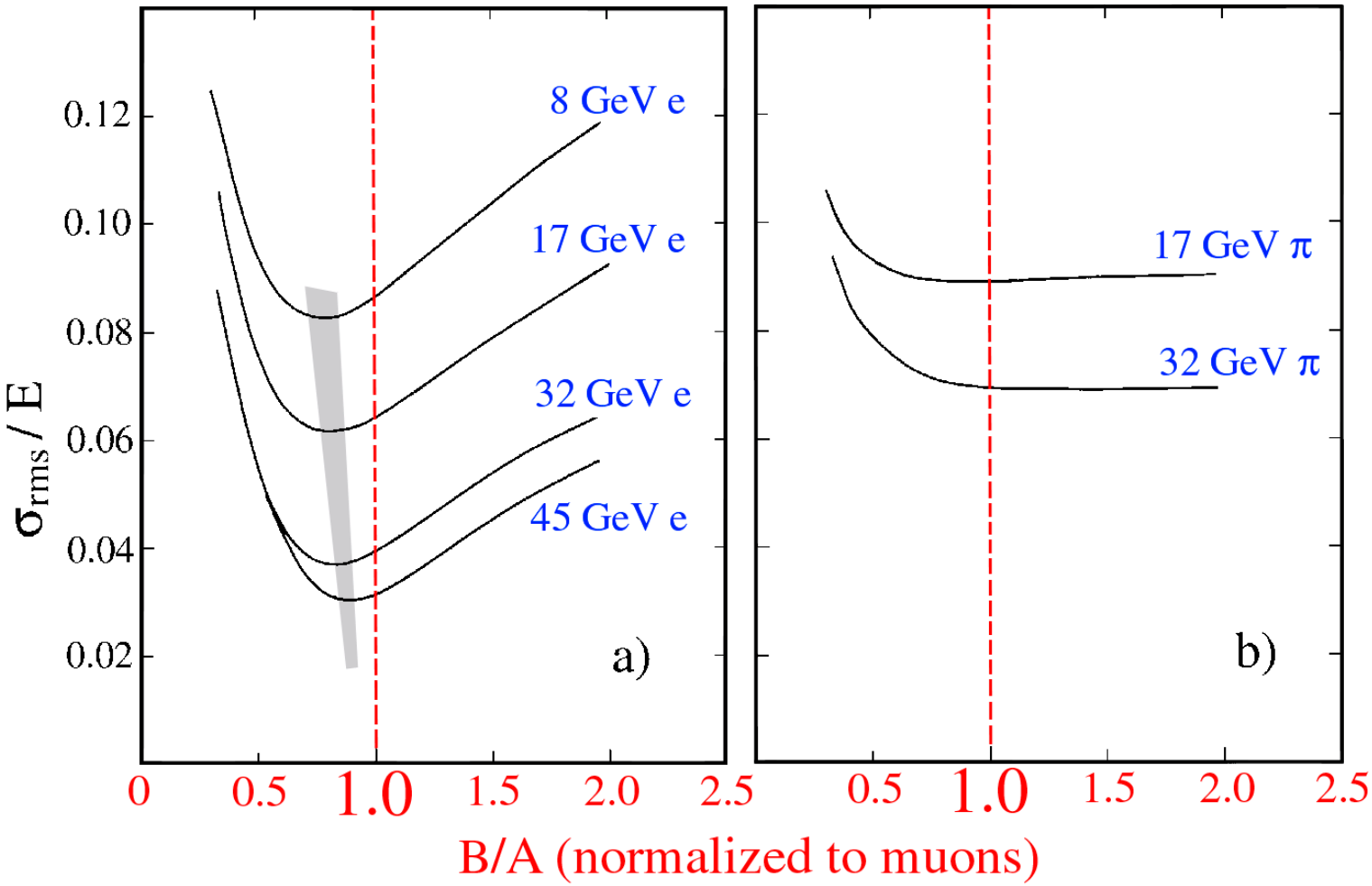


FIG. 6.2. The fractional width $\sigma/E$ of the signal distributions for electrons ($a$) and pions ($b$) of different energies, as a function of the value of the intercalibration constant $B/A$ of the HELIOS calorimeter system. The dashed line corresponds to the intercalibration constant derived from muon measurements [Ake 87].

# Results of miscalibration: Non-linearity

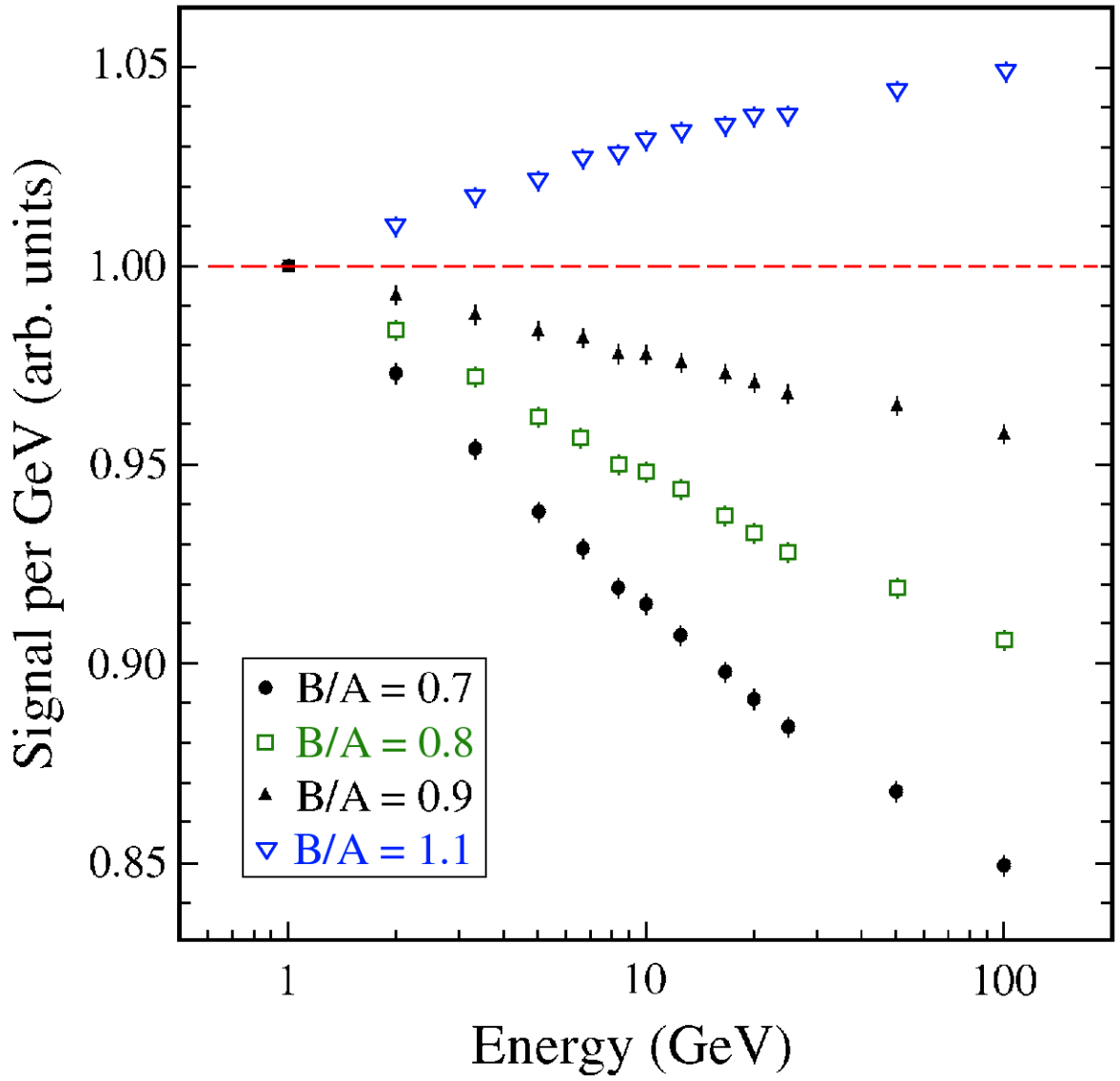


Figure 12: Signal nonlinearity for electrons resulting from miscalibration of a longitudinally segmented calorimeter. The total calorimeter response (average signal per unit of energy) is given for 3 different values of the ratio of the calibration constants for the 2 longitudinal segments, $B/A$. See text for details.

# Results of miscalibration: Mass dependence

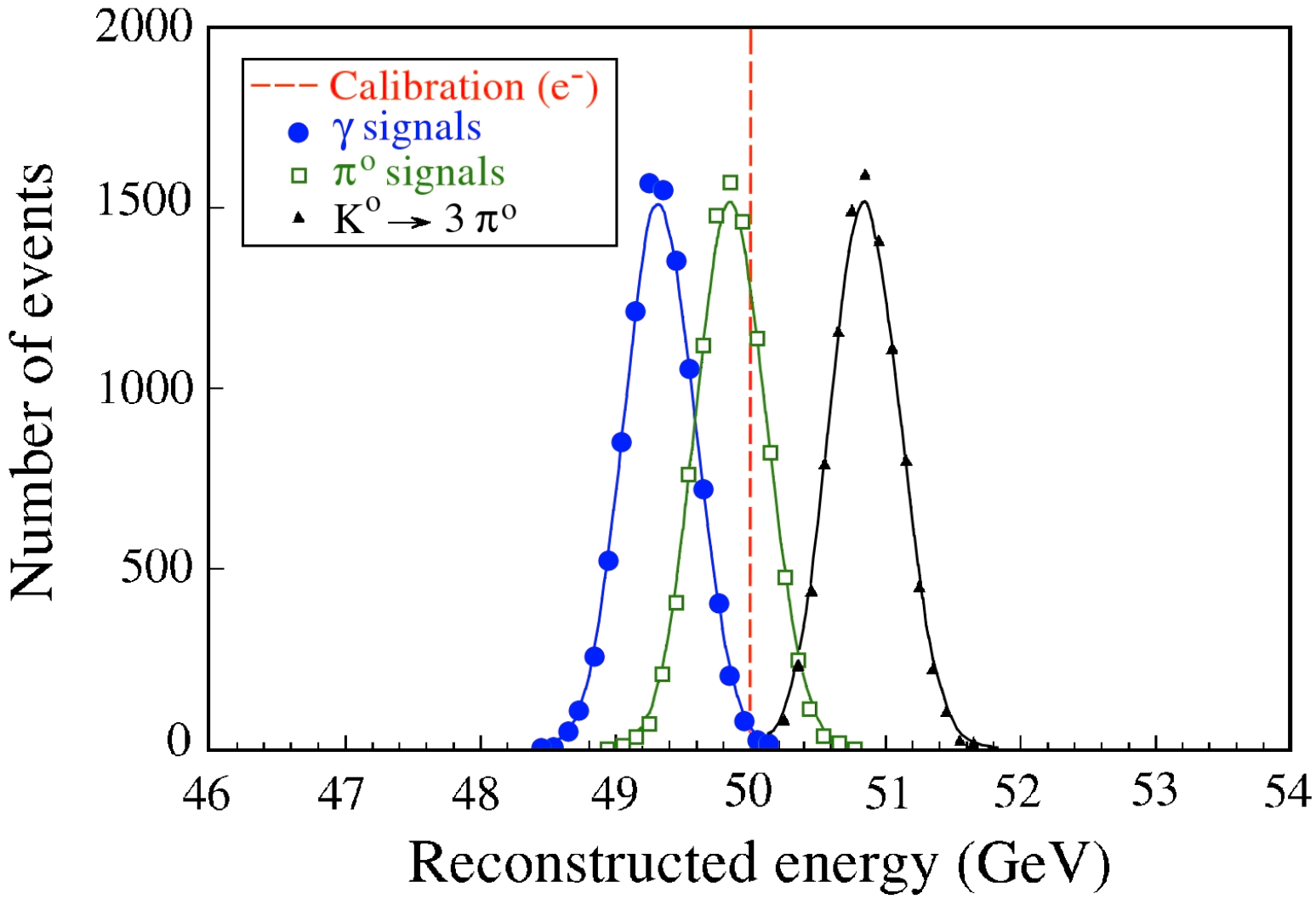


Figure 14: Signal distributions for $\gamma$s and various hadrons decaying into all-$\gamma$ final states. All particles have the same nominal energy and the detector, which has an intrinsic resolution of 0.5% for em showers of this energy, was calibrated with electrons using $B/A = 0.8$. See text for details.

# *Intercalibrating sections by minimizing total signal width*

# GIVES WRONG RESULTS!

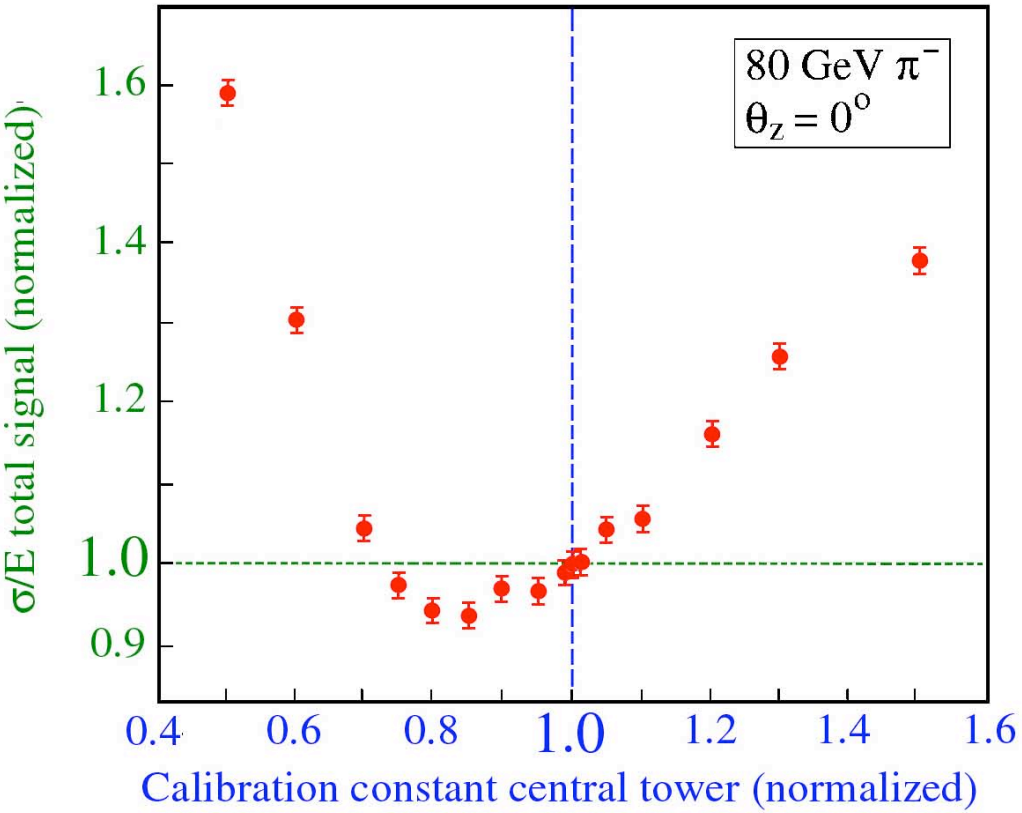


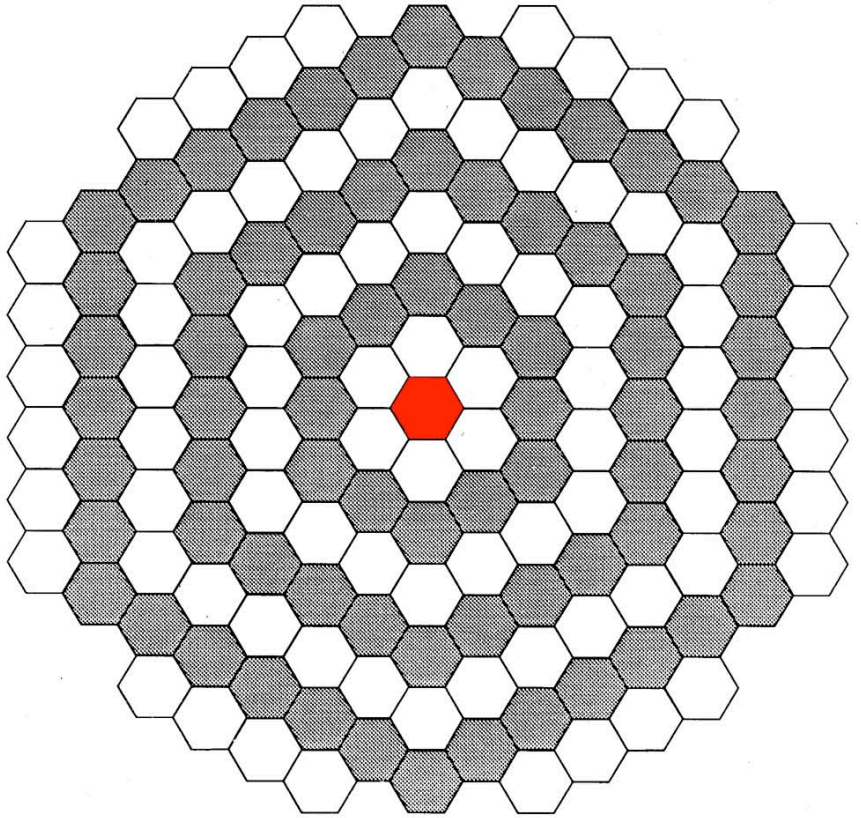

Figure 11: The fractional width, $\sigma/E$, of the signal distribution for 80 GeV $\pi^-$ in the SPACAL detector as a function of the weighting factor applied to signals from the central calorimeter tower into which the pion beam was steered. The calorimeter towers were calibrated with high-energy electrons [7].

From: NIM A485 (2002) 385.

*So what to do?*

- Determine the calibration constants of the longitudinal segments on the basis of

*Monte Carlo simulations !!!*

# *ATLAS: The longitudinally segmented (LAr) ECAL*

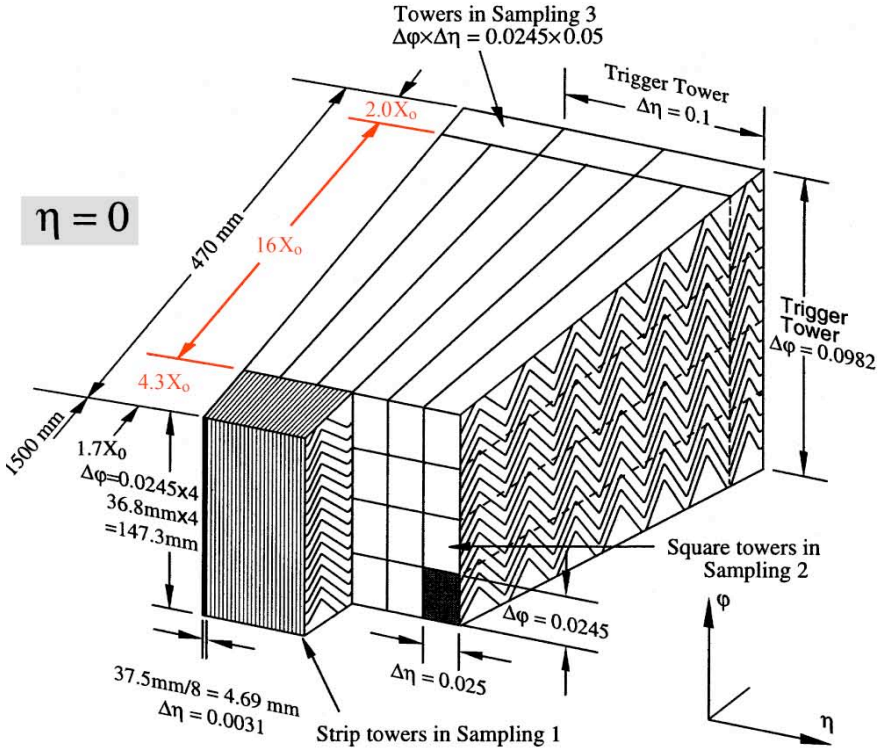


## Depth dependent em sampling fraction

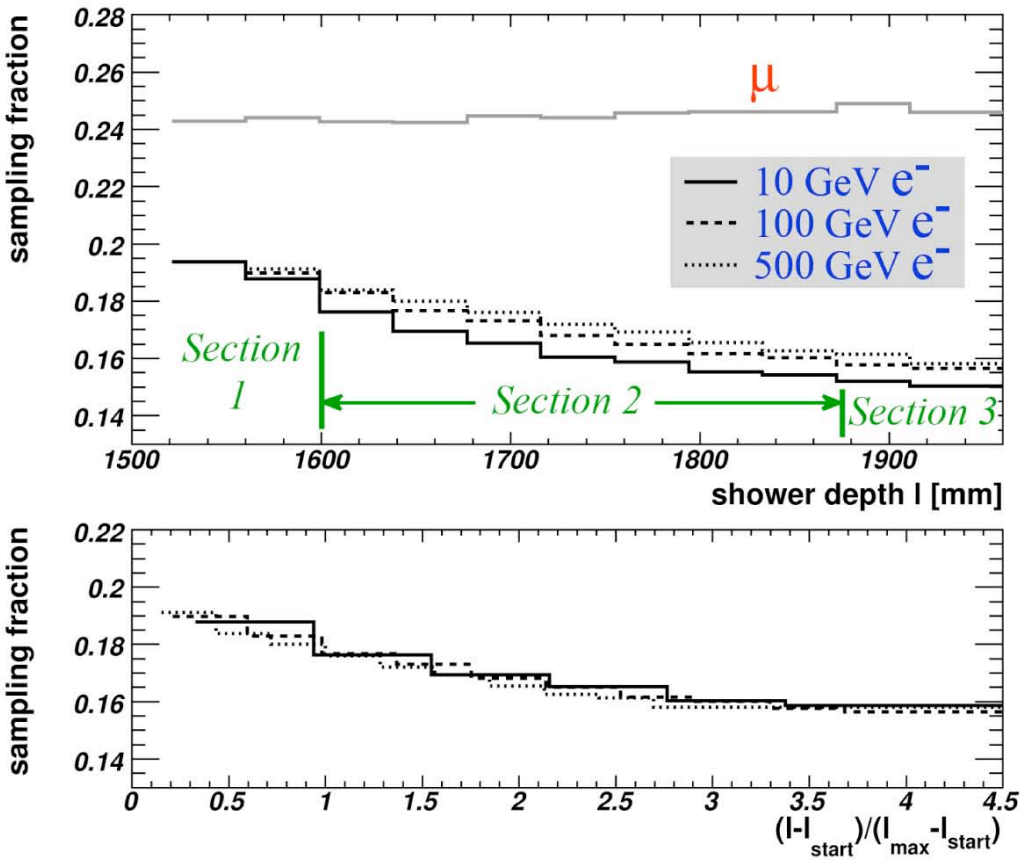

# ATLAS: Energy reconstruction ECAL

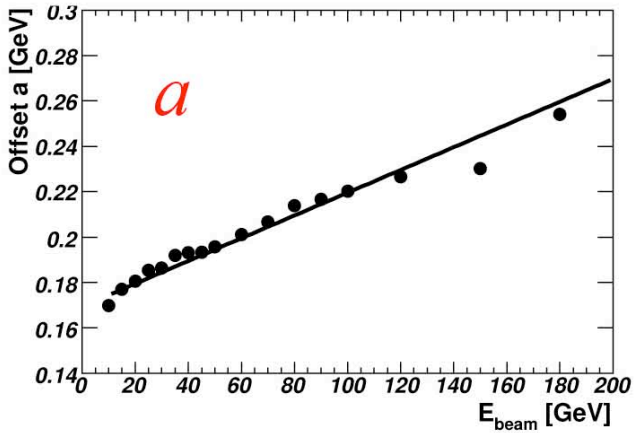


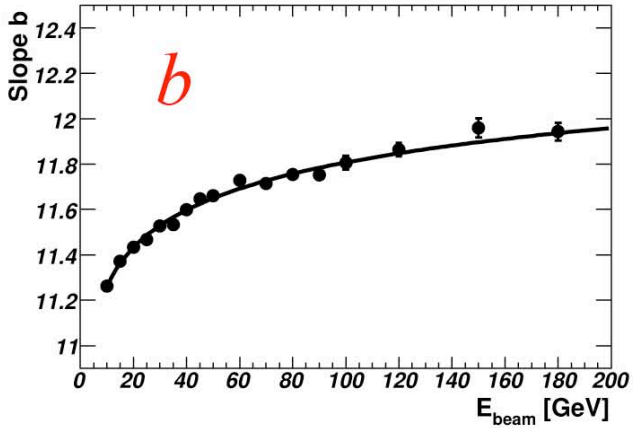


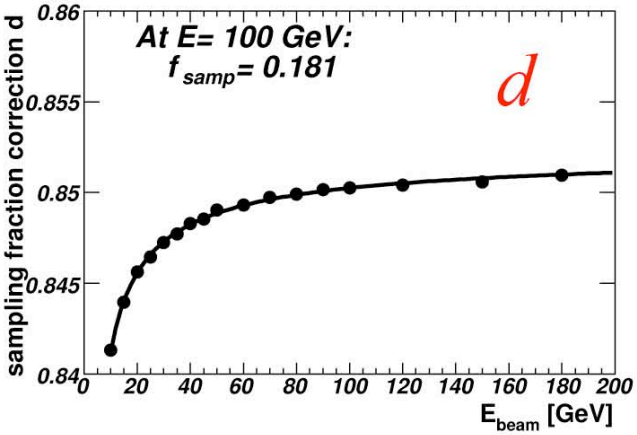


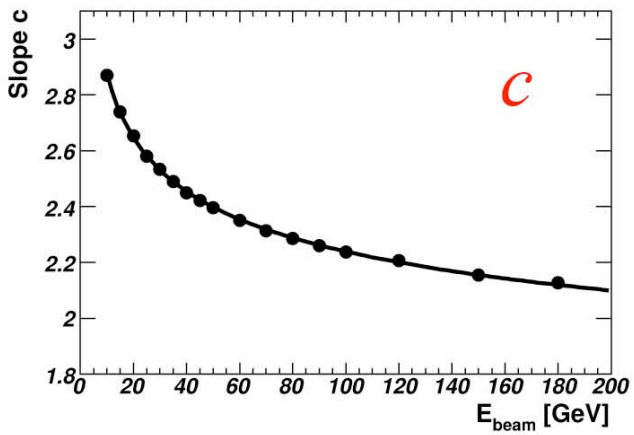


$$E^{rec} = \left( a(E) + b(E)\ E_0^{vis} + c(E)\ (E_0^{vis} \cdot E_1^{vis})^{0.5} + \frac{1}{d(E)\ f_{samp}} \sum_{i=1,3} E_i^{vis} \right) \cdot f_{\text{cell impact}}(\Delta\Phi) \cdot (1 + f_{\text{leakage}})$$

# *e/h*

*factors affecting its value*

# Sampling calorimeters: The e/mip signal ratio

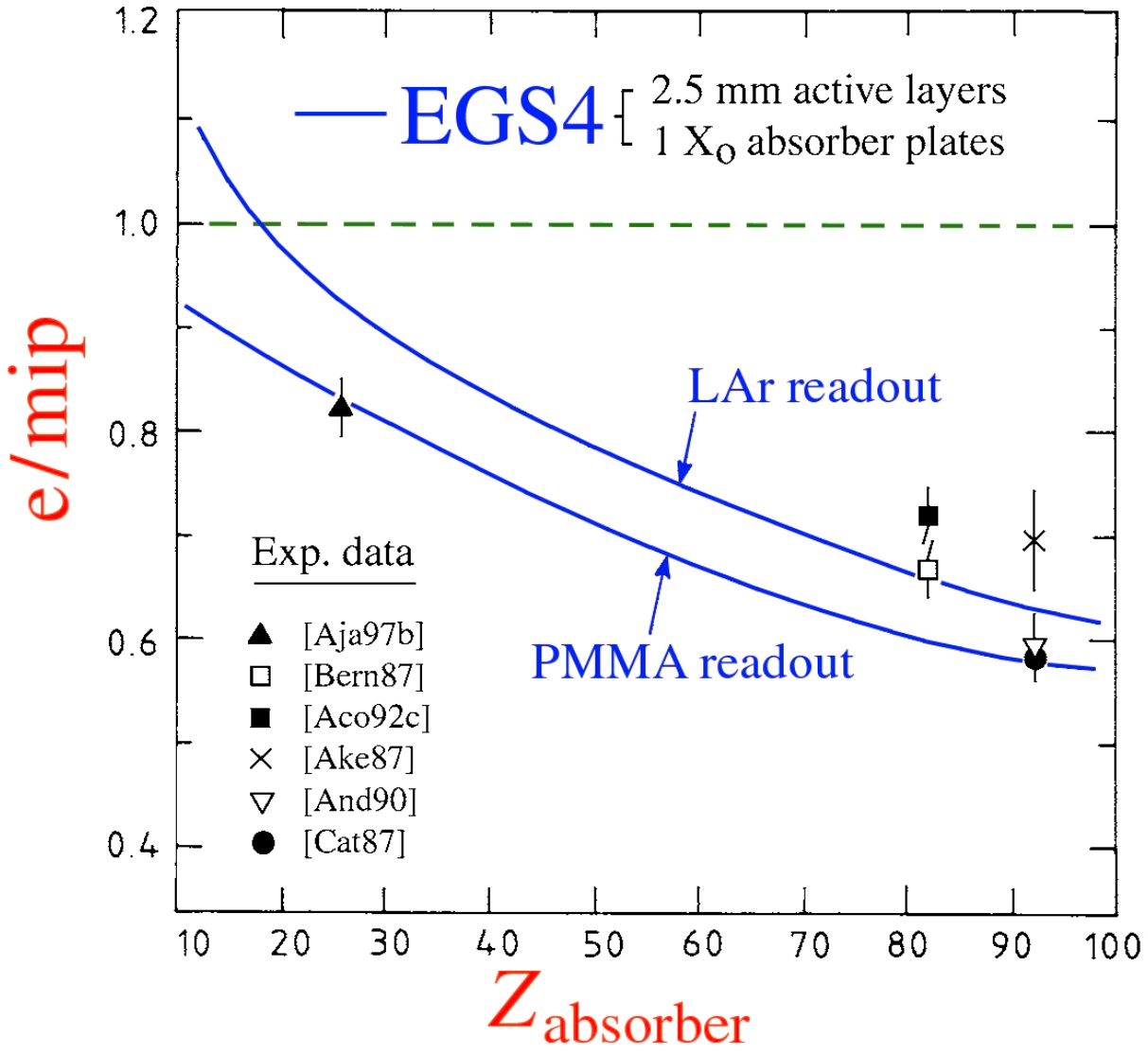


FIG. 3.7. The $e/mip$ ratio for sampling calorimeters as a function of the $Z$ value of the absorber material, for calorimeters with plastic scintillator or liquid argon as active material. Experimental data are compared with results of EGS4 Monte Carlo simulations [Wig 87].

# Aspects of compensation: Sampling of soft shower protons

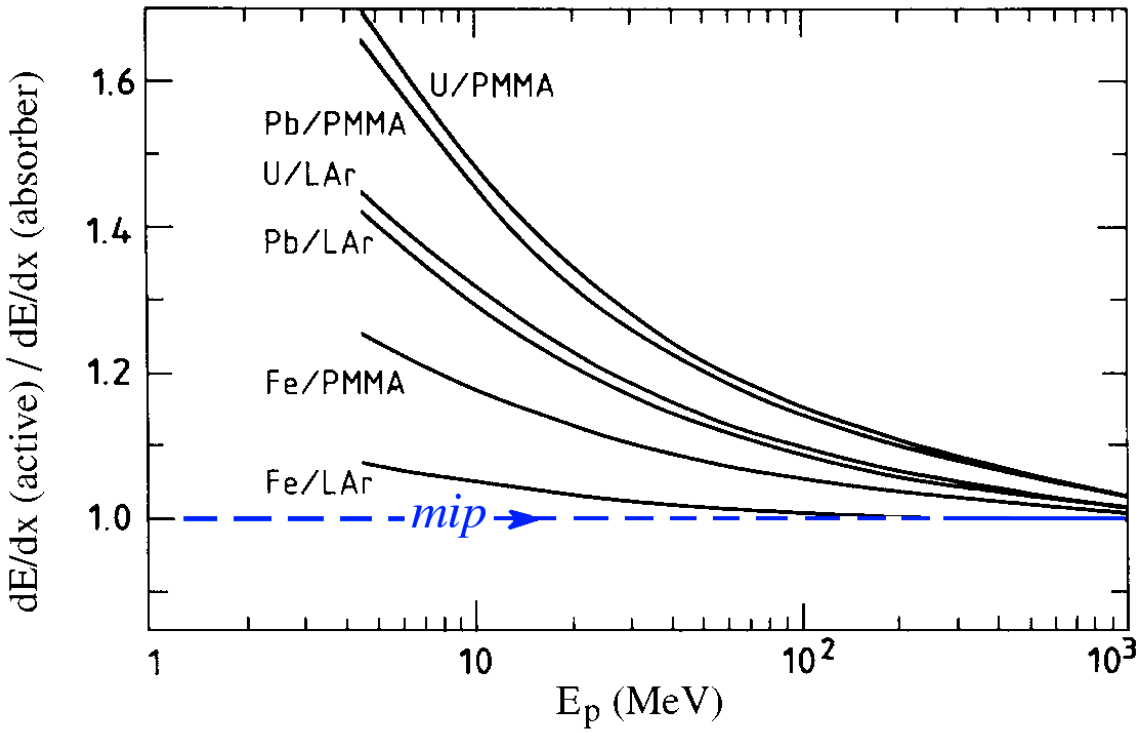


FIG. 3.15. The ratio of energy deposition by non-relativistic protons in the active and passive materials of various calorimeter structures, as a function of the proton s kinetic energy. This ratio is normalized to the one for mips. From [Wig 87].

# Compensation: The spallation proton/mip signal ratio

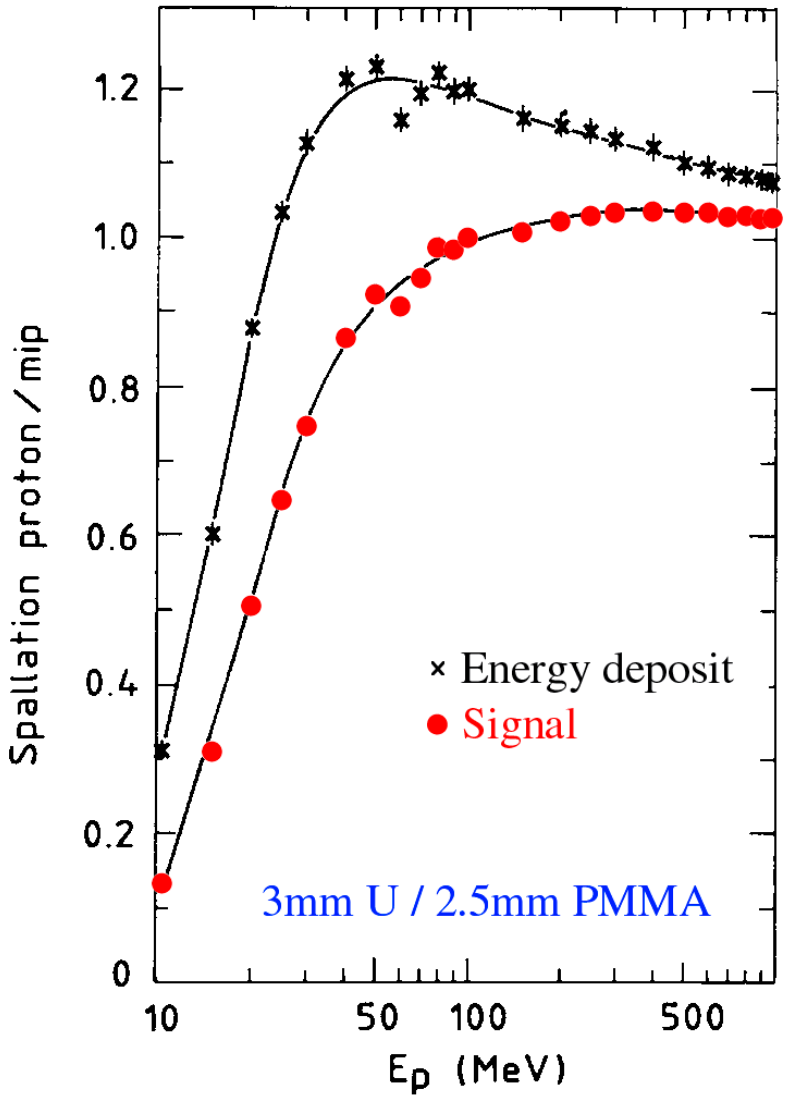


FIG. 3.16. The energy deposit in the active layers (upper curve) and the calorimeter signal (lower curve) for stopping protons, relative to mips, as a function of the kinetic proton energy, in a 3 mm U/2.5 mm PMMA sampling calorimeter. See text for details. Results from Monte Carlo simulations [Wig 87].

# Compensation: The crucial role of the sampling fraction

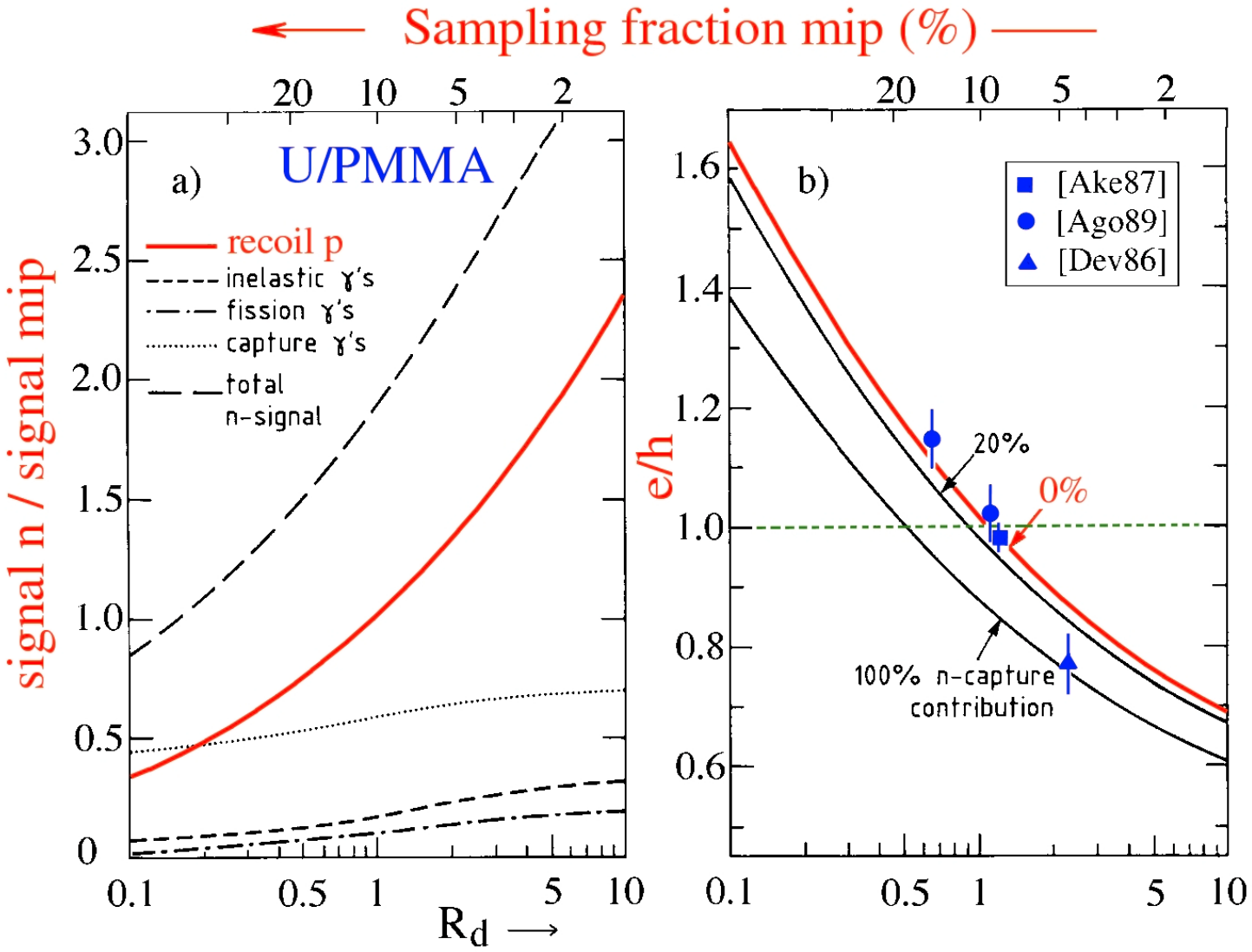


FIG. 3.33. The $n/mip$ response ratio, split up into its components, for $^{238}$U/PMMA calorimeters, as a function of $R_d$, the ratio of the thicknesses of the passive and active calorimeter layers ($a$). The $e/h$ ratio as a function of $R_d$, assuming that 0%, 20% or 100% of the $\gamma$s released in thermal neutron capture contribute to the calorimeter signals ($b$). The top axis of both graphs indicates the sampling fraction for mips. From [Wig 88].

# Compensation in practice: Pb/scintillator calorimeters

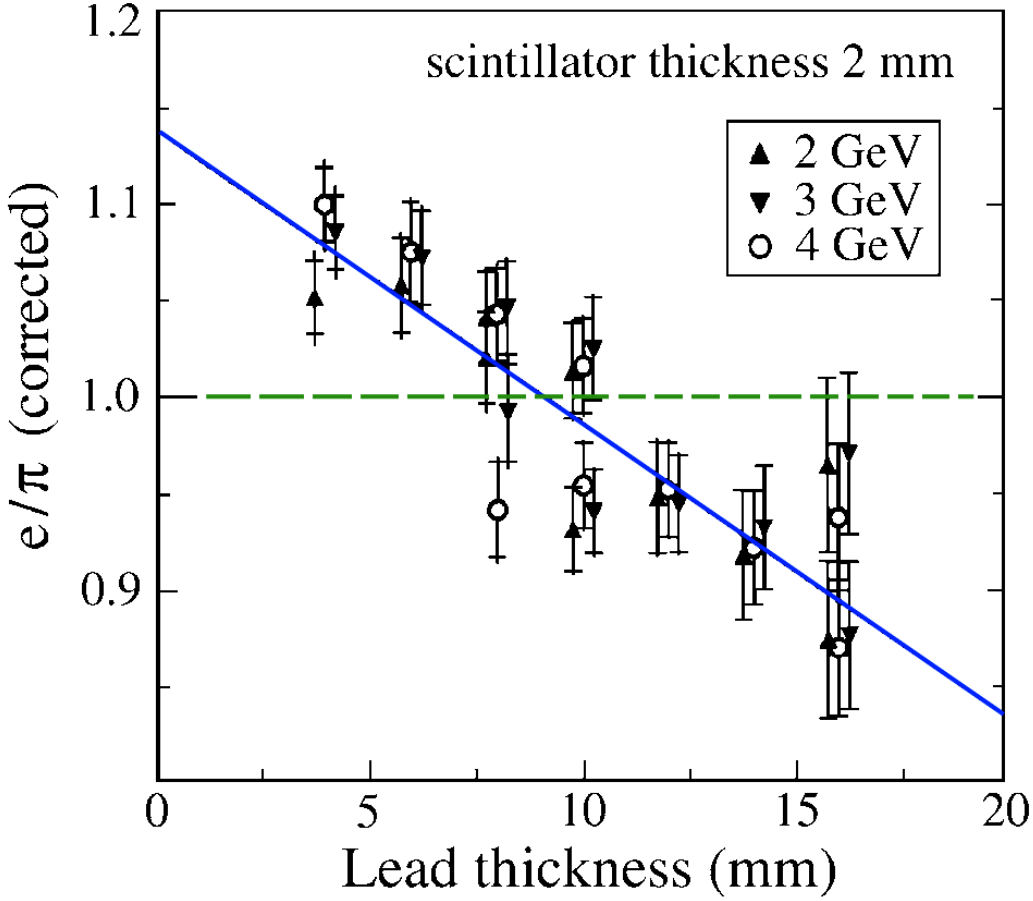


FIG. 3.35. The $e/\pi$ signal ratio, corrected for the effects of shower leakage, for lead/polystyrene-scintillator calorimeters, as a function of the thickness of the lead plates, for 2 mm thick scintillator plates. The inner (outer) error bars show the combined systematic and statistical uncertainty without (with) the shower leakage corrections. The line in the plot is a result of a linear fit to the experimental data [Suz 99].

# Compensation in Fe/scintillator calorimeters?

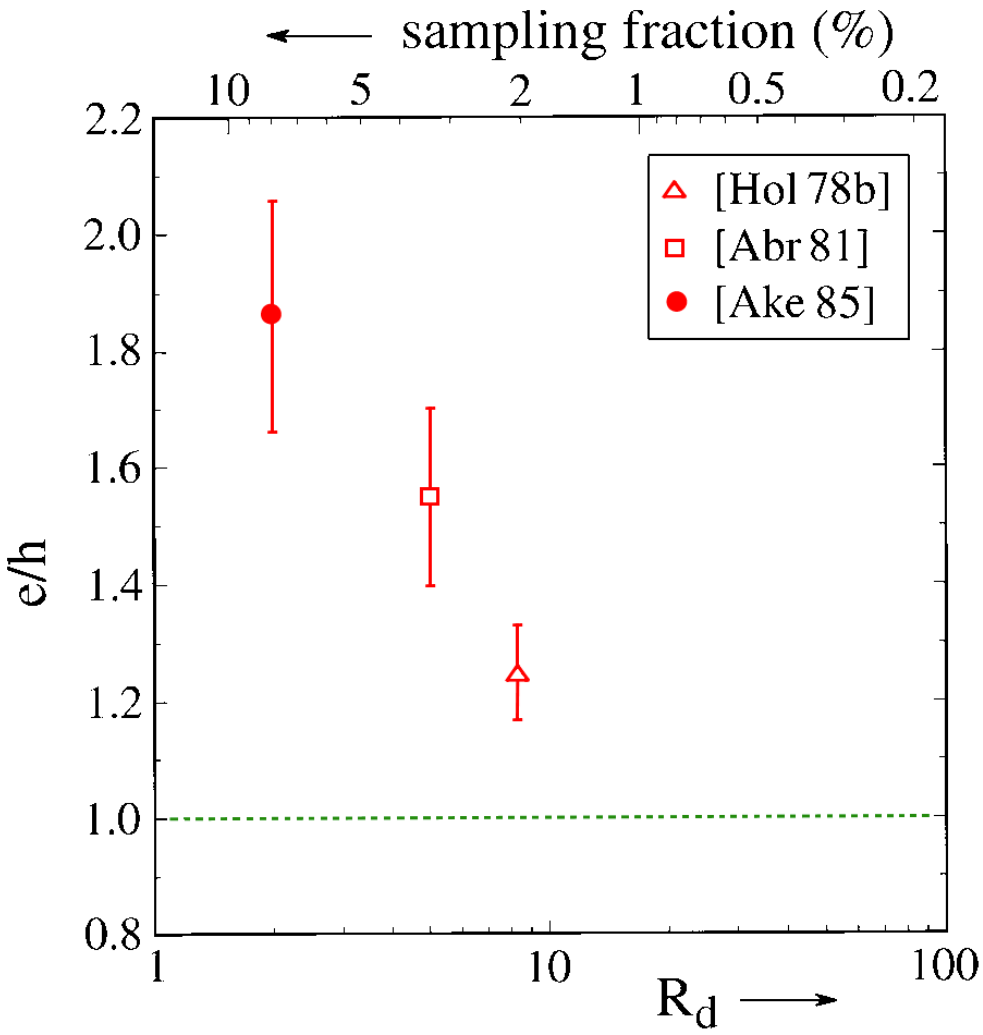


FIG. 3.36. The $e/h$ value for iron/plastic-scintillator calorimeters, as a function of the sampling fraction for mips (top horizontal scale), or the volume ratio of the amounts of passive and active material (bottom horizontal scale).

# Compensation: Slow neutrons and the signal's time structure

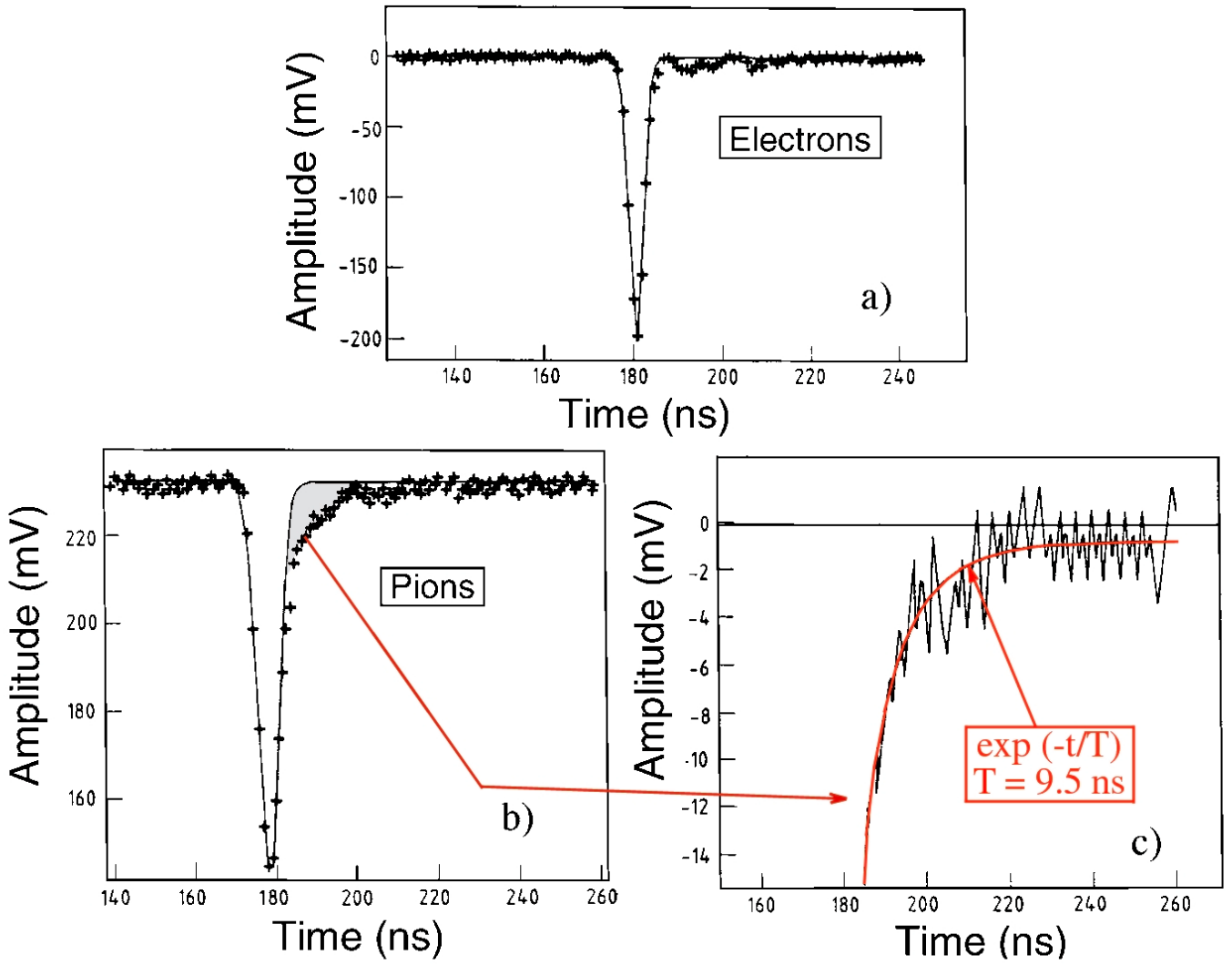


FIG. 3.24. Typical calorimeter signals for 150 GeV electrons ($a$) and pions ($b$) measured with the SPACAL calorimeter. The pion signal exhibits a clear exponential tail with a time constant of $\sim$ 10 ns ($c$). The $t = 0$ point is arbitrary and the bin size is 1 ns. Data from [Aco 91a].

# Compensation: Effect of slow neutrons on the signals

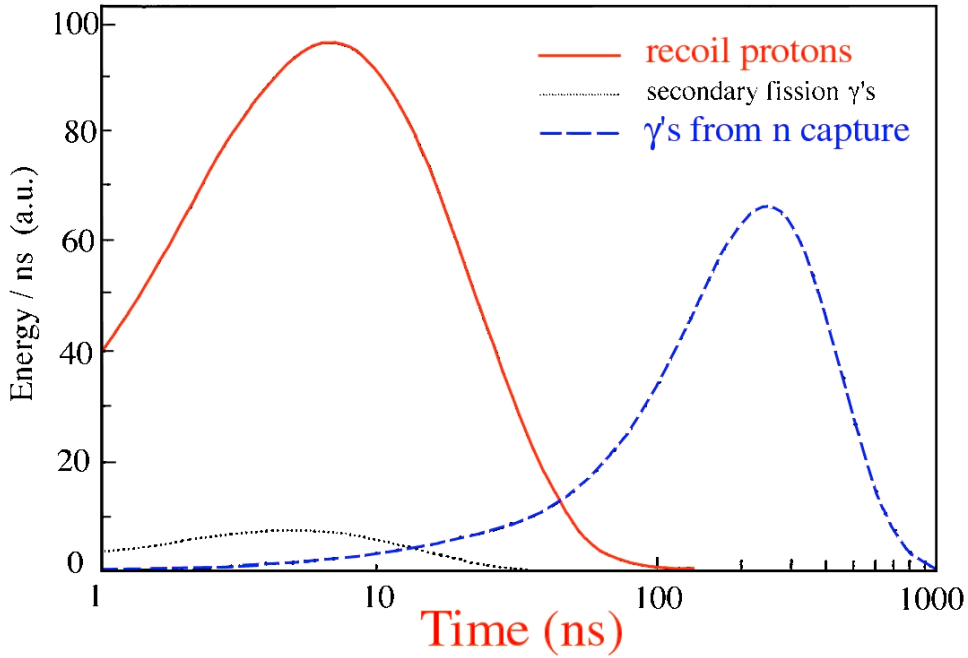


FIG. 3.22. Time structure of various contributions from neutron-induced processes to the hadronic signals of the ZEUS uranium/plastic-scintillator calorimeter [Bru 88].

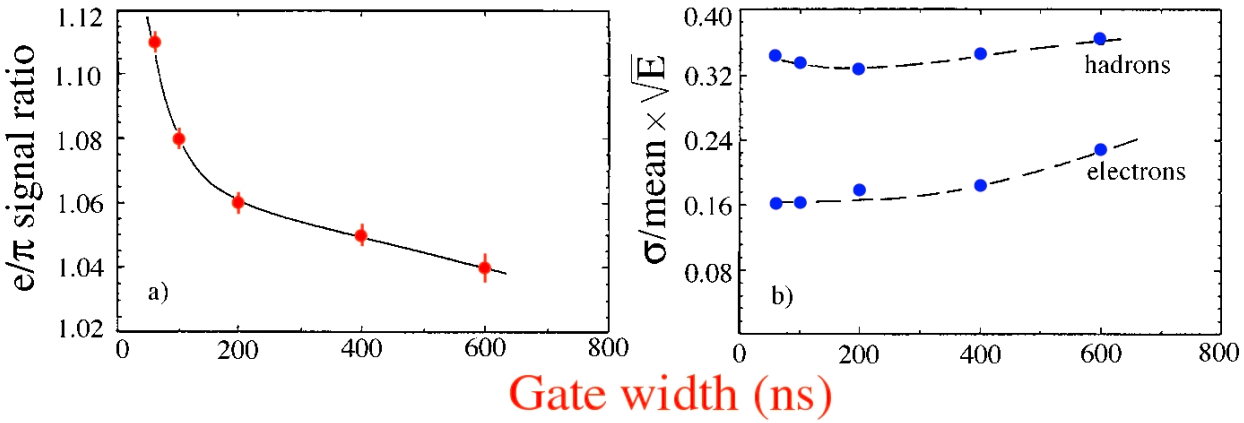


FIG. 3.23. The ratio of the average ZEUS calorimeter signals from 5 GeV/$c$ electrons and pions ($a$) and the energy resolutions for detecting these particles ($b$), as a function of the charge integration time [Kru 92].

# *e/h*

## *its effects on calorimeter preformance*

# *The crucial elements of hadronic shower simulations* (1)

Hadronic showers consist of two distinctly different components:

- An *electromagnetic* component
  ($\gamma$s from $\pi^0$ and $\eta$ decay generate electromagnetic showers)
- A *non-electromagnetic* component
  (The rest)

The main difference (for purposes of calorimetry):

Some fraction of the energy carried by the non-em component does *not* contribute to the calorimeter signals *("invisible" energy)*

Let the *response (average signal per GeV)* to the em component be $e$ and the response to the non-em component $h$

Then, the $e/h$ ratio quantifies this effect

(e.g. in crystal calorimeters, $e/h \sim 2 \longrightarrow$ 50% of non-em energy invisible)

# *The crucial elements of hadronic shower simulations* (2)

## The electromagnetic shower component

Characteristics affecting calorimeter performance in crucial ways

Let $f_{em}$ ($= E_{em}/E_{tot}$) be the *em shower fraction*

| *Characteristic* | *Consequence for calorimetry* |
| --- | --- |
| • $\langle f_{em} \rangle$ increases with energy | Hadronic signal non-linearity |

# *The em shower fraction, $f_{em}$ (1)*

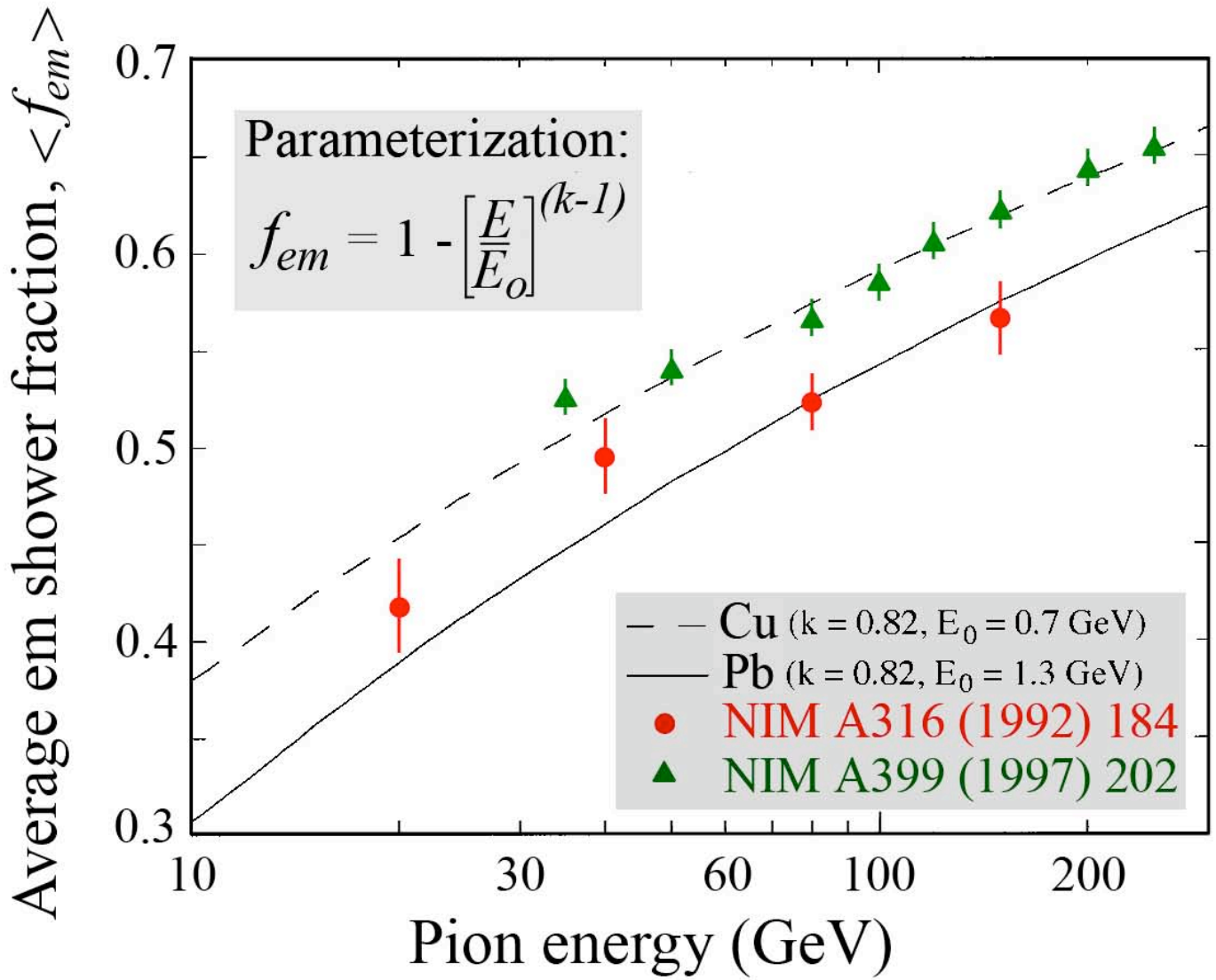


<$f_{em}$> is *large, energy dependent* and *material dependent*

# *The crucial elements of hadronic shower simulations* (2)

## The electromagnetic shower component

Characteristics affecting calorimeter performance in crucial ways

Let $f_{em}$ ($= E_{em}/E_{tot}$) be the *em shower fraction*

| *Characteristic* | *Consequence for calorimetry* |
|---|---|
| • $\langle f_{em} \rangle$ increases with energy | Hadronic signal non-linearity |
| • Fluctuations in $f_{em}$ non-Poissonian | Non-Gaussian response function<br>Deviations from $E^{-1/2}$ scaling |

# *The em shower fraction, $f_{em}$ (2)*

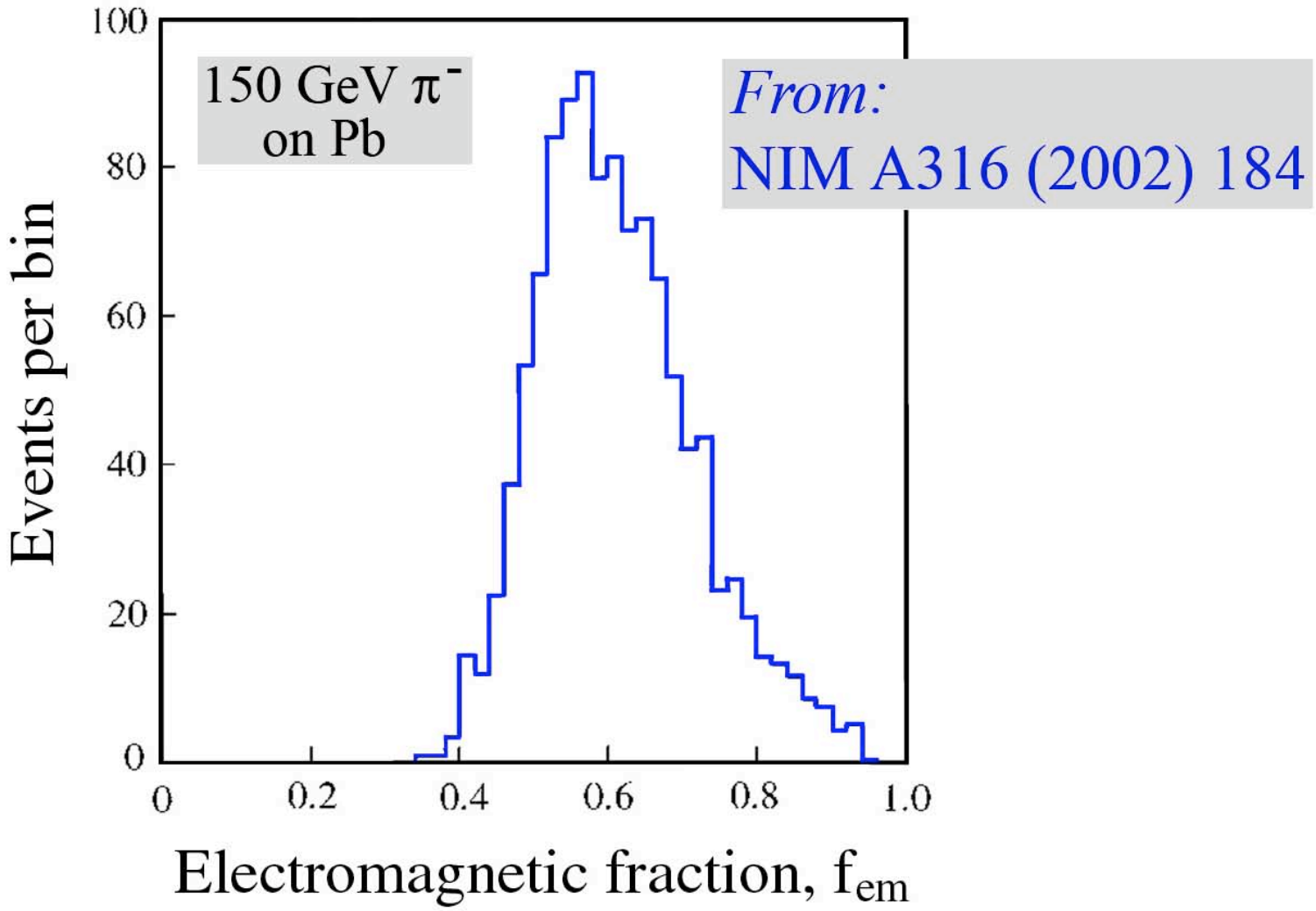


Fluctuations in $f_{em}$ are *large and non-Poissonian*

# Hadronic response function: Effect of e/h

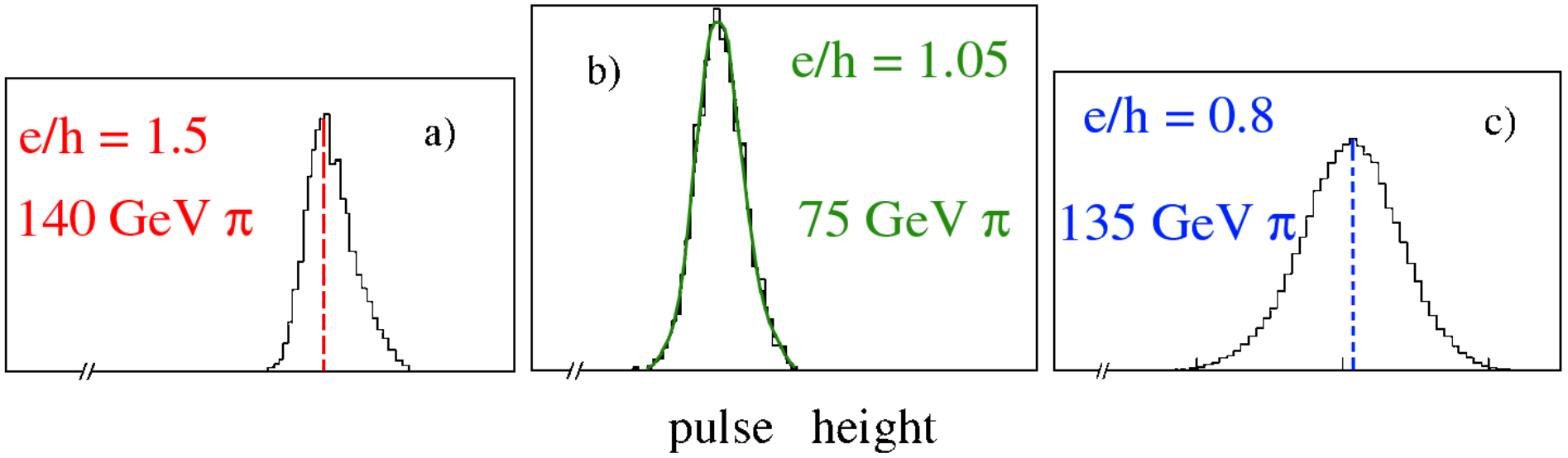


FIG. 7.24. Signal distributions for mono-energetic pions in calorimeters with different $e/h$ values. Data from WA1 [Abr 81], ZEUS [Beh 90] and WA78 [Dev 86].

# *The em shower fraction, $f_{em}$ (3)*

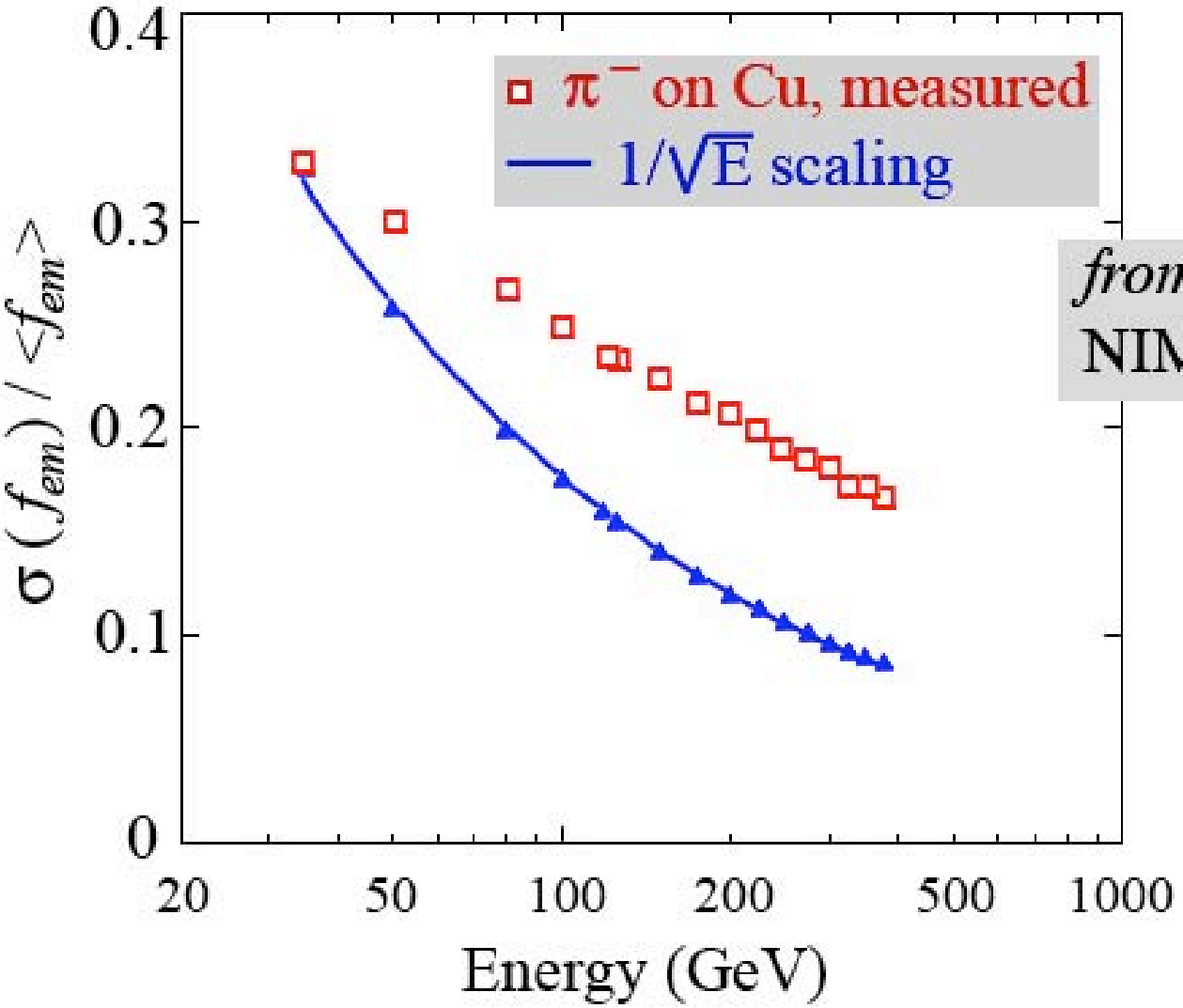


*from*
NIM A399 (1997) 202

Fluctuations in $f_{em}$ are non-Poissonian

# *The crucial elements of hadronic shower simulations* (2)

## The electromagnetic shower component

Characteristics affecting calorimeter performance in crucial ways

Let $f_{em}$ ($= E_{em}/E_{tot}$) be the *em shower fraction*

| *Characteristic* | *Consequence for calorimetry* |
|---|---|
| • $\langle f_{em} \rangle$ increases with energy | Hadronic signal non-linearity |
| • Fluctuations in $f_{em}$ non-Poissonian | Non-Gaussian response function<br>Deviations from $E^{-1/2}$ scaling |
| • Differences between $p$ and $\pi$ | Differences in response<br>Differences in response function |

# *The em shower fraction, $f_{em}$ (4)*

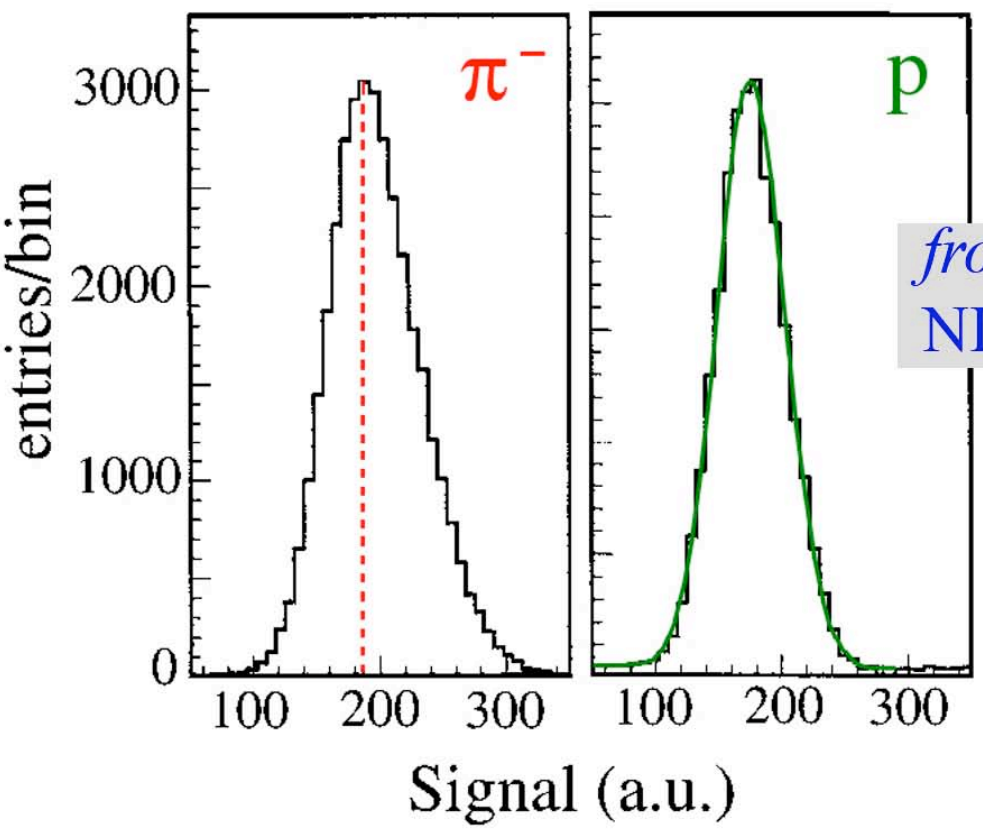


300 GeV showers in Cu

*from:*
NIM A408 (1998) 380

$f_{em}$ fluctuations are different in π- and *p*-induced showers

# The em shower fraction, $f_{em}$ (5)

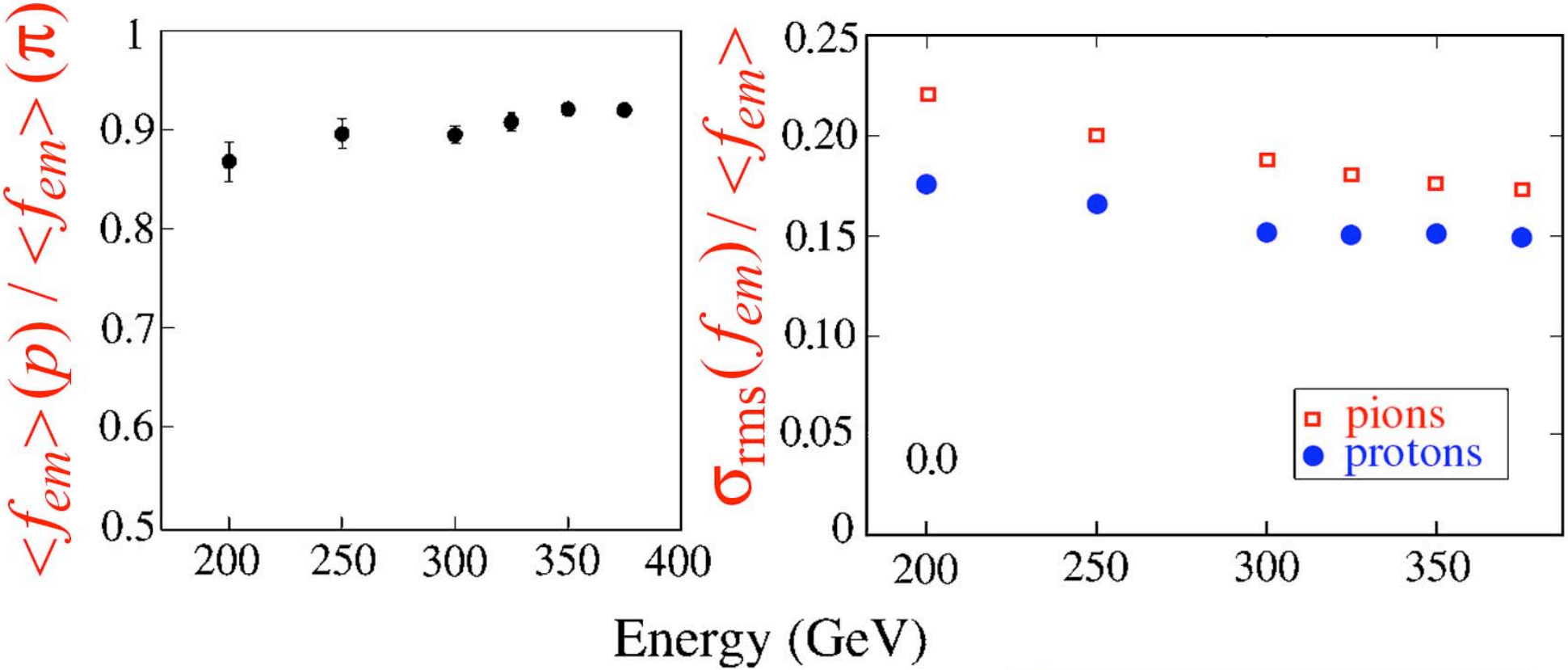


*from:*
NIM A408 (1998) 380

$\langle f_{em} \rangle$ and the fluctuations in $f_{em}$ are different in π- and *p*-induced showers

# *The crucial elements of hadronic shower simulations* (2)

## The electromagnetic shower component

Characteristics affecting calorimeter performance in crucial ways

Let $f_{em}$ ($= E_{em}/E_{tot}$) be the *em shower fraction*

| *Characteristic* | *Consequence for calorimetry* |
|---|---|
| • $\langle f_{em} \rangle$ increases with energy | Hadronic signal non-linearity |
| • Fluctuations in $f_{em}$ non-Poissonian | Non-Gaussian response function<br>Deviations from $E^{-1/2}$ scaling |
| • Differences between $p$ and $\pi$ | Differences in response<br>Differences in response function |
| • Em component distributed over entire shower development | No "characteristic" profiles |

# *"Characteristic" hadronic shower profile does NOT exist*

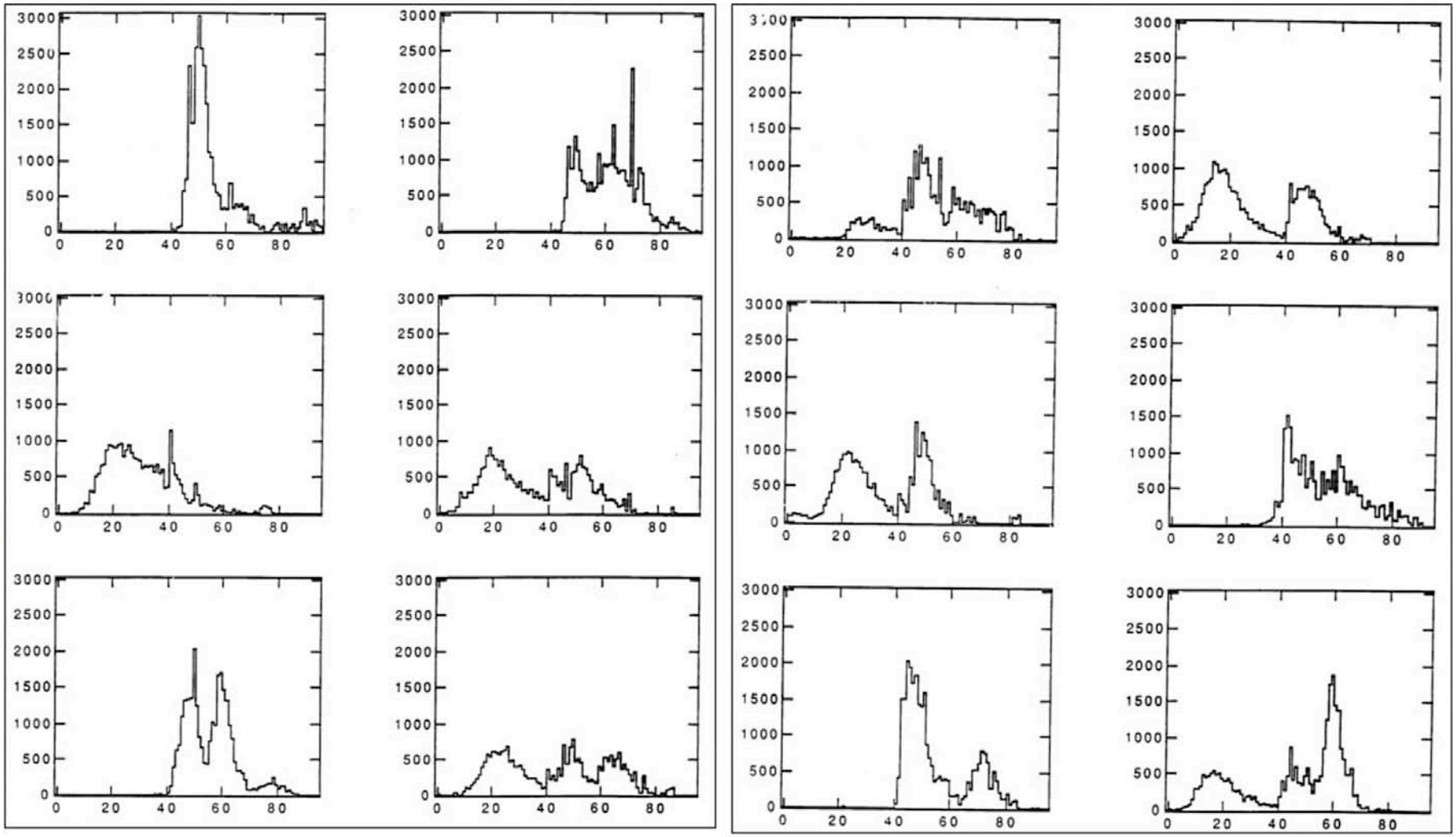


270 GeV π in Pb/scintillator
(hanging-file experiment)

# Pion signals in crystal ECAL + scintillator HCAL

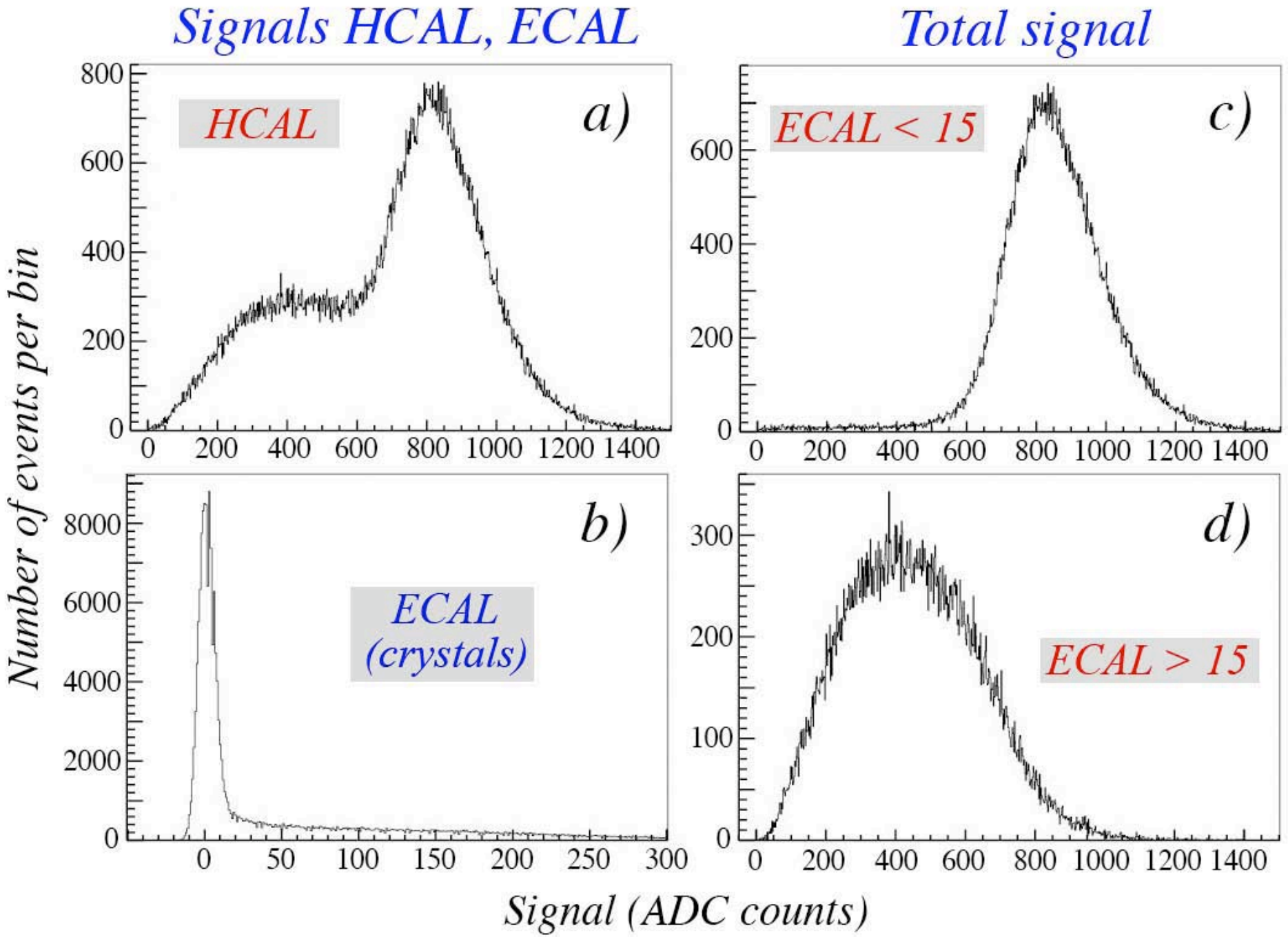

# *Single particles and jets in the CMS calorimeters*

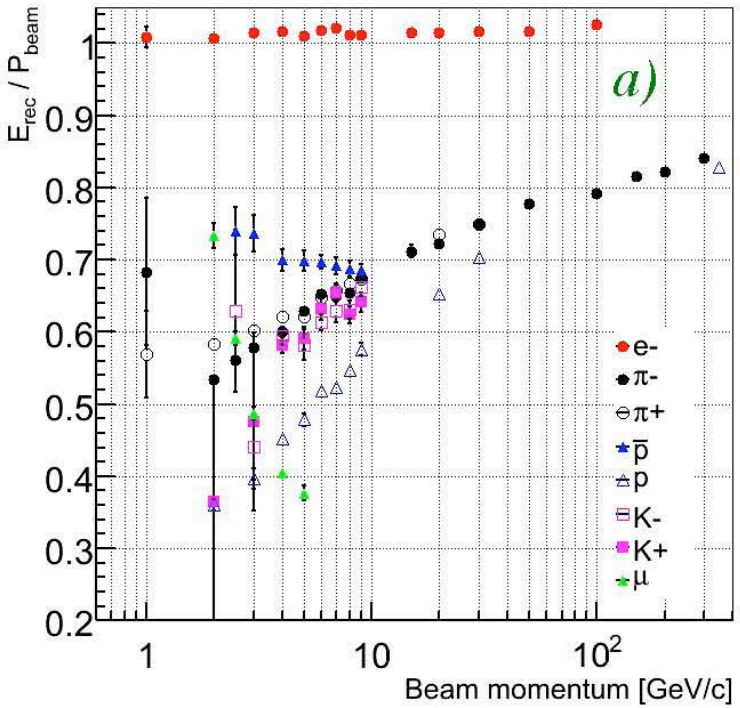


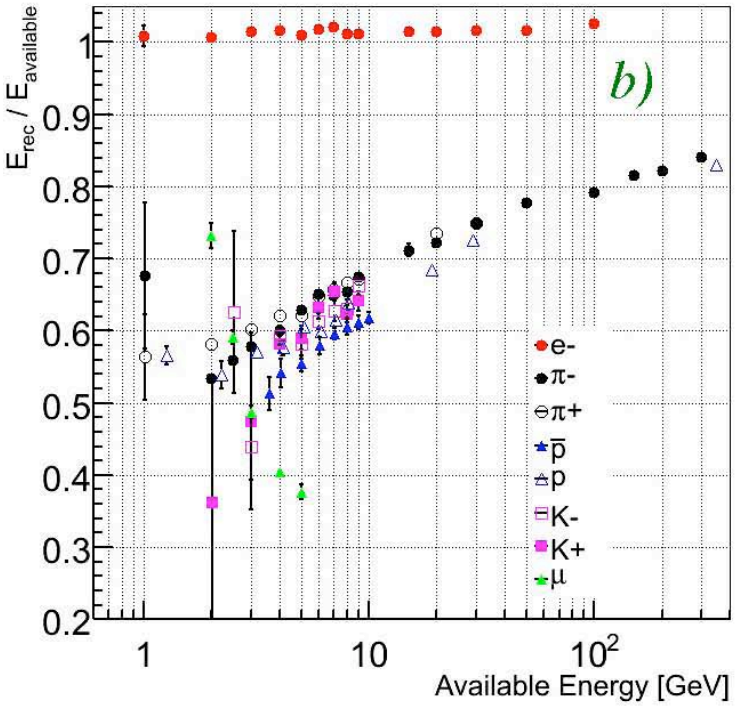


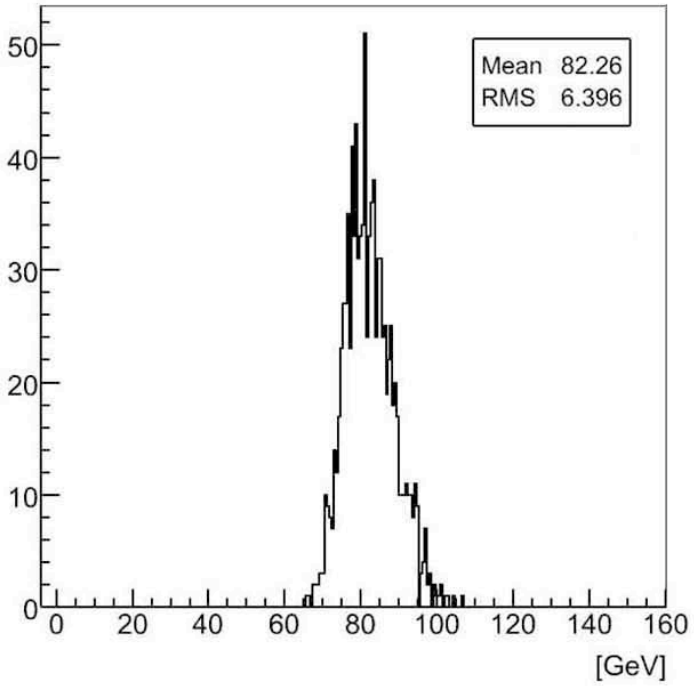


**TB06 reconstructed jet (100GeV)**

*Jet signal reconstructed on the basis of the measured signals from its constituents*

100 GeV jet: σ/mean = 7.8%
(100 GeV π: 11%)

*N.B. Fluctuations in energy sharing between ECAL/HCAL smaller for jets!*